Reliability Engineering and System Safety 257 (2025) 110816

Contents lists available at ScienceDirect

Reliability Engineering and System Safety

journal homepage: www.elsevier.com/locate/ress

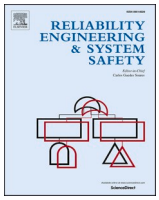

Analysis of system resilience in escalation scenarios involving LH_2 bunkering operations

Federica Tamburini, Matteo Iaiani, Valerio Cozzani *

LISES – Laboratory of Industrial Safety and Environmental Sustainability, Department of Civil, Chemical, Environmental, and Materials Engineering (DICAM), University of Bologna, via Terracini n.28, 40131 Bologna, Italy

ARTICLE INFO

Keywords:
Liquid hydrogen
Bunkering
Resilience assessment
Dynamic Bayesian network
Escalation
Domino effect
Safety barriers

ABSTRACT

In the context of global energy transition and decarbonization efforts, resilience emerges as a critical factor in ensuring the reliability and adaptability of industrial infrastructure systems. This paper introduces a novel model rooted in Dynamic Bayesian Networks (DBNs) for the quantitative assessment of the resilience of engineered systems in the event of escalation scenarios triggered by domino effect. The model is integrated into a systematic, step-by-step procedure capable of evaluating the ability of complex systems to recover functionality from subsequent disruptions occurring at different times throughout the operational lifecycle. Leveraging DBNs, the methodology captures the dynamic interactions and feedback among subsystems or components, overcoming the limitations associated with conventional methods. The innovative methodology has been applied to a case study involving a liquid hydrogen (LH_2) bunkering system, illustrating its effectiveness in assessing resilience amidst evolving accident scenarios. The results demonstrate the significant impact of escalation scenarios on system resilience and underscore the importance of proper implementation and management of safety measures and mitigation strategies. The proposed approach provides a valuable insight into system performance and empowers proactive risk management in the face of escalation scenarios, ensuring the continued operation and success of industrial operations in an uncertain and interconnected reality.

List of Abbreviations & Symbols

BE	Basic Event
BLEVE	Boiling Liquid Expanding Vapor Explosion
BN	Bayesian Network
BOG	Boil-Of-Gas
CCS	Carbon Capture and Storage
CPI	Chemical and Process Industry
CPT	Conditional Probability Table
CTMC	Continuous-Time Markov Chain
DAG	Directed Acyclic Graph
DBN	Dynamic Bayesian Network
EPB	Escalation Prevention Barrier
ERC	Emergency Release Coupling
ESD	Emergency Shut-Down
ET	Event Tree
FP	Failure Probabilities
FRAM	Functional Resonance Analysis Method
FT	Fault Tree
FTA	Fault Tree Analysis
HAZOP	HAZard and OPerability study
He	Helium
HEP	Human Error Probability
HFB	Human Factor Barrier
HRA	Human Reliability Analysis
IPB	Ignition Prevention Barrier
LH_2	Liquid Hydrogen
LNG	Liquified Natural Gas
LTS	Land To Ship
M&OB	Management & Organizational Barrier
MCMC	Markov Chain Monte Carlo
MLE	Maximum Likelihood Estimation
MLI	Multi-Layer Insulation
MTBF	Mean Time Between Failure
MTTR	Mean Time To Repair
NHCTMC	Non-Homogenous Continuous-Time Markov Chain
PRAF	Process Resilience Analysis Framework
PSF	Performance Shaping Factor

* Corresponding author.
E-mail address: valerio.cozzani@unibo.it (V. Cozzani).

https://doi.org/10.1016/j.ress.2025.110816
Received 4 August 2024; Received in revised form 5 January 2025; Accepted 9 January 2025
Available online 13 January 2025

PSV	Pressure Safety Valve
QCDC	Quick Connect Disconnect Coupler
RDB	Release Detection Barrier
RIPSHA	Resilience-based Integrated Process Systems Hazard Analysis
RPB	Release Prevention Barrier
RPT	Rapid Phase Transition
SB	Safety Barrier
SH_2IFT	Safe Hydrogen Fuel Handling and Use for Efficient Implementation
SHIPP	System Hazard Identification, Prediction and Prevention
SPAR-H	Standardized Plant Analysis Risk-HRA
STAMP	System-Theoretic Accident Model and Processes
STS	Ship To Ship
TTF	Time To Failure
TTS	Truck To Ship

1. Introduction

In the dynamic landscape of global energy transition, resilience emerges as a pivotal concept, addressing the challenges and opportunities presented by the shift towards sustainable and renewable energy sources [1]. In the effort to mitigate the impacts of climate change and reduce carbon footprint, the integration of new technologies becomes essential [2]. Carbon Capture and Storage (CCS) technology along with hydrogen-based systems represent two of these potential innovative solutions [3]. However, this transformative journey is not without risks [4,5]. In fact, the rapid adoption of innovative solutions, also including smart grids, artificial intelligence, and decentralized energy systems, introduces a host of emerging challenges [6]. These challenges include cyber threats, technological disruptions, and increased vulnerabilities within interconnected infrastructure [7–9]. In the face of these complexities, the imperative for new strategies and methodological frameworks to improve resilience is evident [10]. Resilience, in the context of energy transition, involves the ability of systems to anticipate, prepare for, respond to, and recover from disruptions, ensuring a reliable energy supply [11,12]. This approach not only safeguards against potential threats but also fortifies the energy sector to withstand the uncertainties associated with the energy transition process [1].

In the maritime sector, with increasing emphasis on decarbonization and the adoption of alternative fuels, such as LNG (liquified natural gas), LH_2 (liquid hydrogen), and biofuels, the infrastructure dedicated to bunkering operations must adapt to accommodate for these changes [13]. Consequently, significant investments in new technologies, infrastructure upgrades, and regulatory frameworks supporting the safe and efficient supply of alternative fuels are imperative [14]. Resilience in this context involves not only the physical infrastructure, but also the ability to anticipate and respond to market dynamics, regulatory shifts, and technological advancements [15]. The evaluation of resilience within maritime bunkering operations emerges as a new area of research as industries seek to mitigate risks and enhance operational stability in the face of disruptions [16].

In addition, the Oil&Gas sector, as well as the chemical and process industry, is susceptible to escalation scenarios, which are events in which a primary accident propagates involving one or more secondary equipment with resulting consequences more severe than the previous ones [17,18]. Alternative names used to define this kind of events are “domino” or “knock-on” accidents [19,20]. Indeed, several escalation scenarios have been observed among process equipment, pipelines, and other critical infrastructure [21,22]. About 5754 significant marine domino accidents were collected from IMO and HIS Markit [23]. Although there have not yet been any reported accidents in the marine bunkering operations of LH_2, primarily due to the limited number of active infrastructure nowadays [24], escalation scenarios are deemed possible as well given the aforementioned evidence of domino effect in the offshore energy infrastructure [23].

A recent literature review addressing resilience methods in the chemical and process industry (CPI) highlighted several resilience assessment methodologies available to handle uncertainties, disturbances, and potential hazards [25]. These methodologies include approaches such as the Functional Resonance Analysis Method (FRAM) [26–29], the Process Resilience Analysis Framework (PRAF) [30], the Bayesian network (BN) model [31], the System-Theoretic Accident Model and Processes (STAMP) [32], and the Resilience-based Integrated Process Systems Hazard Analysis (RIPSHA) [33]. While these approaches have been widely applied to CPI complex systems, limited research is available concerning the resilience assessment of systems in the event of escalation scenarios [10]. Only a few studies addressed the topic. However, they have primarily approached it from a qualitative or semi-quantitative perspective and within specific application domains [6,34–37]. For instance, Cincotta et al. [36] proposed a method which delved into domino accidents, but within the context of fire safety and firefighting intervention operations. A more generic approach was proposed by Chen et al. [37]. However, the numerical method proposed shows some limitations in addressing the possibility of escalation scenarios occurring at different times throughout the entire operating process. On the contrary, Tan et al. [38] developed a methodology to assess the resilience of multi-state systems over time, but they assumed a discrete state of the system, not accounting for continuous state systems.

Based on previous findings, it is possible to assert that time represents a further crucial factor when dealing with resilience evaluations [27,28,39]. A resilience perspective might indeed consider how a system can flexibly adapt to unexpected disruptions, for example, by rapidly adjusting production processes or re-routing materials in response to disruptions from process unit failures, human errors, cyber-physical attacks, and natural hazards, among others [40–44].

Furthermore, within the aforementioned approaches, only few studies addressed resilience assessment in the context of maritime infrastructure [45–49]. To the best of the author’s knowledge, only Vairo et al. [45] and Claussner and Ustolin [49] published research studies on resilience in cryogenic fuels bunkering operations. Vairo et al. [45] proposed a dynamic model based on Bayesian inference and Markov Chain Monte Carlo (MCMC) simulations to be applied to LNG bunkering operations, while Claussner and Ustolin [49] proposed a qualitative framework for assessing system resilience applied to LH_2 storage facilities.

In the present study an innovative conceptual model is introduced for the quantitative assessment of the resilience of engineered systems over time in the event of escalation scenarios. A step-by-step procedure is also provided to support the application of the developed model to investigate how a complex infrastructure withstands or recovers from subsequent disruptions occurring at different times throughout the operational lifecycle (resilience assessment). The novel procedure provides a systematic and explicit tool applicable to evaluate the resilience of different complex systems. The approach relies on a Dynamic Bayesian Network (DBN). This allows overcoming the limitations associated with state-of-the-art methods, such as fault trees (FTs) and event trees (ETs), which often overlook dynamic interactions and feedback among subsystems or components [39]. To demonstrate the effectiveness of the novel approach developed, an application to a notional case study involving a liquid hydrogen bunkering system potentially susceptible to escalation scenarios across an extended period of time was carried out.

The following part of the paper is structured as follows. In Section 2, the quantitative resilience assessment methodology developed to address escalation scenarios is presented, also introducing the relevant features of Dynamic Bayesian Networks and the resilience metrics adopted. Section 3 illustrates the case study of interest for the application of the developed approach, involving an offshore LH_2 bunkering system, while Section 4 presents the outcomes of the application. Finally, results are discussed in Section 5 and some conclusive remarks are outlined in Section 6.

2. Methodology

The original approach developed in the present study to support the quantitative assessment of resilience of engineered systems over time in the event of escalation scenarios, based on a DBN model and a specific resilience metric, is presented in the following. The relevant features of DBNs are first introduced, then the resilience metric is presented. The quantitative model for resilience assessment and the procedure for its application are then illustrated in detail.

2.1. Dynamic Bayesian network

A Dynamic Bayesian network (DBN) is an advanced probabilistic graphic model that extends the principles of Bayesian networks (BNs) to accommodate temporal dependencies within dynamic systems [10,50]. At its core, a DBN is a representation of a joint probability distribution over a set of random variables at different time steps. It is particularly applicable in scenarios where the state of a system evolves over time (e.g., sensor validation, risk management, environmental modelling, etc.), and understanding the temporal dynamics is crucial for making informed predictions [51–53].

The DBN framework involves a directed acyclic graph (DAG) where nodes represent random variables and arcs encode conditional dependencies between them [54]. Nodes can be categorized into parents and child nodes. Arcs are directed from parent to child nodes. The nodes that are not linked to any parent node are called root nodes while the ones without any outcoming arcs are defined as leaf nodes. Marginal prior probabilities are assigned to root nodes while the relational logic between two or more intermediate and leaf nodes is defined through associated Conditional Probability Tables (CPTs) [55].

To formalize the temporal aspect, each node in the graph is associated with a specific time point, indicating the evolution of the system over discrete time steps. The joint probability distribution is found not only by multiplication of the node probabilities in the same time step, as done when handling static BNs, but also considering the nodes and their connections in the previous time steps, as follows [10]:

$$P(X_{1:T}) = P(X_1)\prod_{t=2}^{T} P(X_t|P_a(X_t)) \tag{1}$$

where X_t denotes the random variable at time t, $P_a(X_t)$ represents the set of parents of X_t in the DAG, $X_{1:T}$ indicates the set of random variables from time 1 to T, and the conditional probabilities $P(X_t|P_a(X_t))$ capture the dynamic relationships between the current state X_t and its parents $P_a(X_t)$ at time t [56].

If new data becomes available, probabilistic reasoning and updating beliefs can be performed using the Bayes' theorem, as follows:

$$P(X|E) = \frac{P(X)\cdot P(E|X)}{P(E)} \tag{2}$$

where $P(X|E)$ is the posterior probability of node X given evidence E (i.e., the new observation) [54].

In the present study, given the features described above, DBNs have been selected to model the probability of the system functionality in case of occurrence of escalation scenarios over time.

2.2. Resilience metrics adopted

In the last decades, several resilience metrics have been proposed with the aim of assessing the ability of an engineered system to face disruptions. Unlike many existing methods assess resilience based on the impact of undesired disruptions in terms of performance loss, Tong et al. [10] redefine resilience by adopting a functionality term [57,58]. Resilience, in their context, is measured by assessing the probability of a system functionality state sustaining a "high" state or restoring to a "high" state from a "low" state during and after disruptions within a specific time frame [10]. Thus, Tong and coworkers [10] consider the resilience as the sum of the normal operating and restored states of the system as previously meant by Yodo et al. in [59]. This time-dependent probabilistic definition provides a comprehensive perspective, considering both temporal and probabilistic characteristics of resilience. Therefore, the metric introduced by Tong et al. [10] has been adopted in the present study to model the resilience of the system.

The metric relies on the definition of four resilience attributes, which are pivotal elements within a resilient system: absorption, adaptation, restoration, and learning [60]. Absorption is the inherent ability of a system to endure and withstand disturbances. It is particularly crucial when disruptions are inevitable, as it helps to mitigate the decreasing rate of functionality. Adaptation refers to the capability of a system to adjust to a disrupted environment, recovering lost functionality without relying on external restoration efforts. Restoration represents the ability of a system to facilitate external interventions aimed at repairing damage caused by disturbances, ultimately restoring it to a new state of normality. The functionality of the new state can be either higher or lower than that of the pre-disruption state, as long as system operation is guaranteed. Finally, learning is a dynamic attribute that involves enhancing future system responses to disturbances by integrating past experiences. The contribution of all these elements to the resilience of a system can be visualized in Fig. 1-a), where the time-dependent resilience model in terms of functionality curve of a system is reported [10]. As shown, four states are used to quantify resilience. Notations such as $S1$ (normal operating state with functionality $F1$ when a disruption occurs at t_0), $S2$ (disrupted state with functionality $F2$), $S3$ (state with functionality $F3$ after adaptation), and $S4$ (new stable state with functionality $F4$ after restoration) are introduced to illustrate these states. Learning ability impacts the functionality variation over the entire period.

The ability of the system to absorb, adapt, restore, and learn throughout each phase determines the transition rates between the states (λ_1, λ_2, μ_1, μ_2). The high or low functionality that characterize the resilience attributes (based on the inherent degradation rate of the system and the loss of system functionality after the disruption) also influence the values of the transition rates. In Tong et al. [10], the Markov chain model has been adopted to illustrate this concept (see Fig. 1-b)). In order to model the resilience, the Markov chain model has been transformed into a DBN (see Fig. 1-c)). The transition probabilities of each state are converted into the conditional probabilities of node "*State of functionality*" given the resilience attributes. Thus, resilience can be quantified as the sum of the probabilities of state $S1$ and $S4$ at each time step.

Overall, the functionality curve offers a dynamic portrayal of how a resilient system responds to disruptions over time, emphasizing the interconnectedness of absorption, adaptation, restoration, and learning in maintaining and improving the system functionality. Indeed, according to Tong et al.'s [10] definition of resilience provided above, examining resilience means analyzing changes in system functionality. Therefore, in the present study, the temporal variations in system functionality due to the occurrence of escalation scenarios after a disruption are considered to assess the overall resilience of the system under analysis.

2.3. The resilience escalation model

Engineered systems are subjected to process accidents, defined as sequences of events initiated by the deviation of process parameters, failures, or malfunctioning of one or more components [17]. These accidents can result in different level of consequences, ranging from a near miss, which is an event that does not result in actual loss but has the potential to do so, up to a catastrophic disaster, which is an event that could cause multiple fatalities and extensive damage to assets and production [61]. Within this category of accidents, those involving chains of

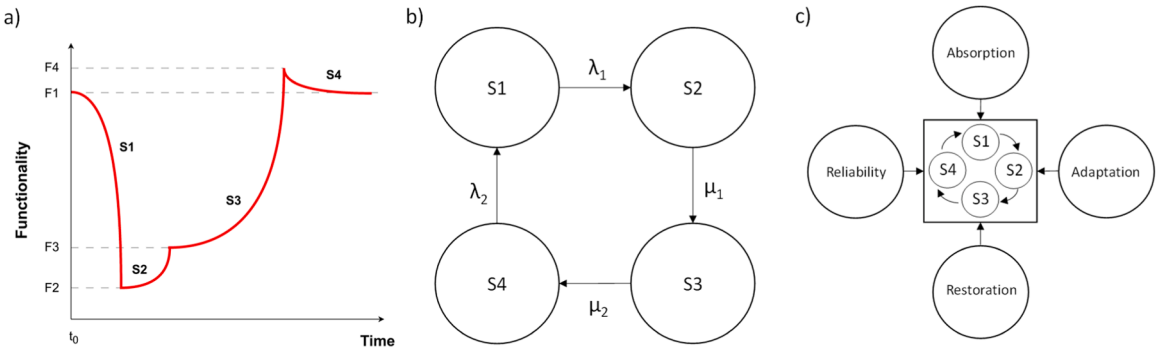

Fig. 1. a) Time-dependent functionality curve under a single disruption ($S1$, normal operating state with functionality $F1$ when a disruption occurs at t_0; $S2$, disrupted state with functionality $F2$; $S3$, state with functionality $F3$ after adaptation; $S4$, new stable state with functionality $F4$ after restoration); b) Markov chain model; c) DBN resulting from the conversion of the Markov chain model (adapted from [10]).

accidents in which a primary undesired event (disruption event) sequentially or simultaneously triggers one or more secondary undesired events (escalation scenarios) in nearby equipment or facilities, leading to consequences of the secondary accidents more severe than those associated with the primary disruption event, are termed "escalation accidents" or domino effects [17,62].

In the present section a resilience metric has been proposed to account for the potential occurrence of escalation scenarios over time, derived from that originally proposed by Tong et al. [10]. Specific original definitions are introduced for the functionality states, and novel approaches are developed to obtain a specific Markov chain model, to carry out the DBN construction, and to build the corresponding resilience curve for the system.

2.3.1. Definition of functionality states in the event of escalation scenarios

The number of functionality states needed to assess the system resilience in the event of a domino effect depends on the possible number of escalation scenarios taking place. Let $[n]$ denotes the set $\{1, \ldots, N\}$, where i represents the index for the i^{th} escalation scenario affecting the system. In this context, $(S2_i)_{i\in[n]}$, $(S3_i)_{i\in[n]}$, and $(S4_i)_{i\in[n]}$ denote the new states introduced to characterize the system functionality following each escalation scenario. These states supplement $S1$, $S2$, $S3$, and $S4$, which describe the functionality of the system during a single disruption event.

Fig. 2 illustrates the resilience model developed in the present study, based on the functionality curve approach, adapted to accommodate N escalation scenarios. The overall trend in system functionality in the case of N escalation scenarios is represented by the red curve in Fig. 2. The curve corresponds to the functionality curve of the model by Tong et al. [10], shown in Fig. 1-a), which addresses a single disruption event. While it is assumed that the first disruption event occurs when the system is in a high functionality state (i.e., the system is in $S1$ at t_0), the state of system functionality when a new escalation scenario occurs is characterized by uncertainty. In fact, a probability distribution is associated with the possible states of system functionality, and the actual state following the accident depends on the sequence of events occurred before and during the escalation scenario under consideration, leading to its final outcome. For this reason, the points on the resilience curve in Fig. 2 which would correspond to the occurrences of the escalation scenarios after the first disruption (i.e., the points where a drop in system functionality takes place) are actually represented through dashed circles in order to express the uncertainty behind the states of functionality when an escalation scenario occurs, as was previously discussed. This issue is further discussed in Section 2.3.3, when describing the Markov chain for system functionality modelling [63].

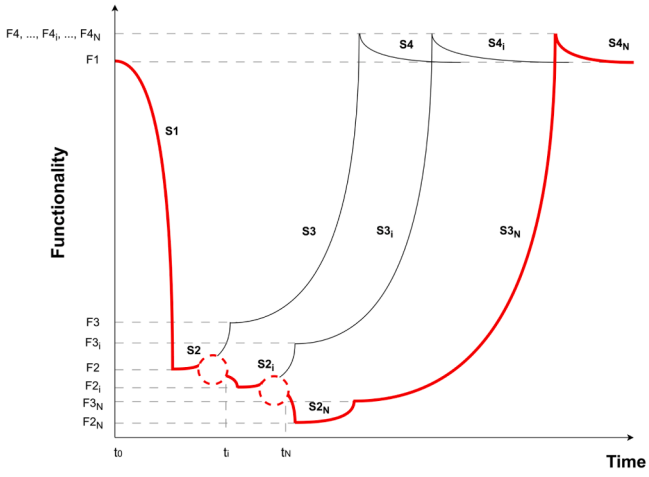

Fig. 2. Time-dependent functionality curve in the event of N escalation scenarios after a disruption event.

2.3.2. Resilience metrics in the event of escalation scenarios

According to the definition of resilience of Tong et al. [10], the resilience of a system can be calculated based on the probability of the system to be in a high functionality state, i.e., the state ($S1$), or in a recovered state after a single ($S4$) or more than one escalation scenarios ($S4$ and $(S4_i)_{i\in[n]}$).

In the case of generalization to N escalation scenarios after a disruption, resilience can be quantified as the sum of the probabilities of states $S1$, $S4$, and $(S4_i)_{i\in[n]}$ that have been calculated as a function of time by the DBNs computation:

$$R = S1 + S4 + \sum_{i=1}^{N} S4_i \tag{3}$$

2.3.3. Markov chain model in the event of escalation scenarios

On the basis of the new states of functionality introduced in Section 2.3.1 to account for N escalation scenarios, a novel Markov chain model has been developed to assess the transitions from one state to another. Its conceptual representation is shown in Fig. 3-a), where *Block 0* resembles the Markov chain proposed by Tong et al. [10] (single disruption scenario) (see Fig. 1-b)), while *Block i* and *Block N* represent the Markov chains of the i^{th} escalation scenario and the N^{th} escalation scenario (the last occurring), respectively. As shown in Fig. 3-a), the transition probabilities (i.e., λ and μ) among the states change at each block, reflecting alterations in resilience attributes (absorption, adaptation, restoration, and learning) due to the different accidental events occurring. The only exception is λ_2, expressing the degradation reliability of the entire system, which is an inherent characteristic that may be considered to be unaffected by external disturbances. If λ_1, λ_2, μ_1, and μ_2

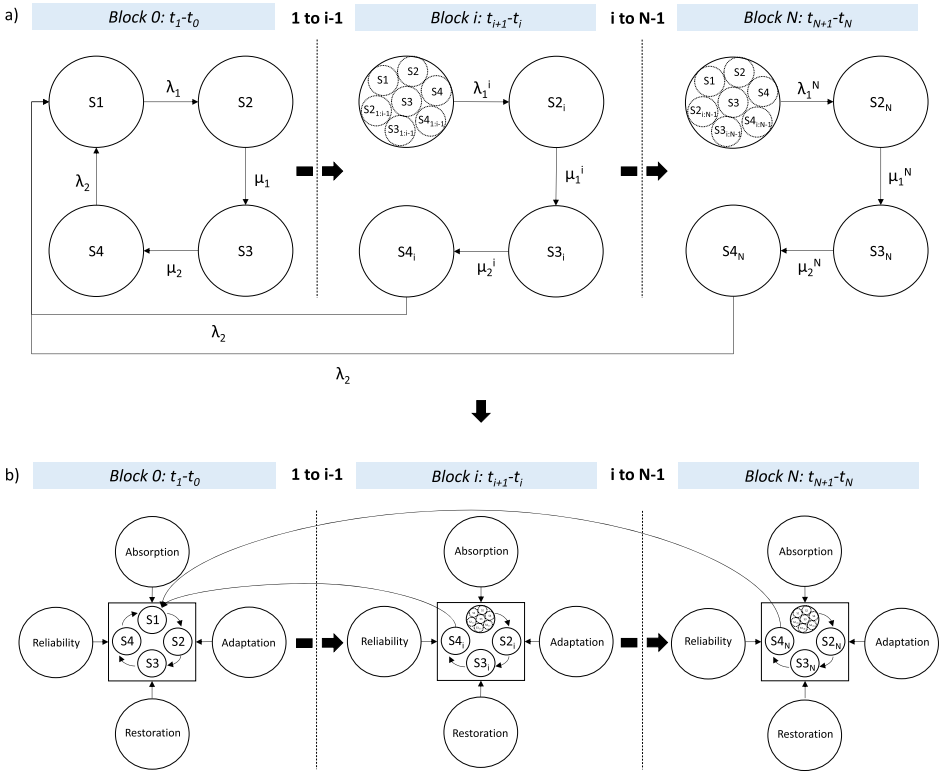

Fig. 3. The Markov chain model transformation into DBNs in the event of N escalation scenarios: a) the proposed novel Markov chain model; b) the DBNs resulting from the conversion of the novel Markov chain model.

are the transition rates associated with the first disruption (see *Block 0* in Fig. 3-a) and Fig. 1-b)), $(\lambda_1^i)_{i\in[n]}$, $(\mu_1^i)_{i\in[n]}$, $(\mu_2^i)_{i\in[n]}$ and λ_2 denote the transition rates associated with each escalation scenario (see *Block 0 and Block N* in Fig. 3-a)). It should be recalled (see Section 2.3.1) that the state of system functionality when a new escalation scenario occurs is uncertain. Thus, probability distributions are associated with the states of system functionality. This concept is visually represented through multiple dashed circles in blocks i and N of Fig. 3-a), with each circle corresponding to a potential state of system functionality. For instance, the state of functionality of the system when the i^{th} escalation scenario occurs can be one of the following: $S1$, $S2$, $S3$, $S4$, $(S2_{1:i-1})_{i\in[n]}$, $(S3_{1:i-1})_{i\in[n]}$, or $(S4_{1:i-1})_{i\in[n]}$.

The resilience attributes may be in either a high (H) or low (L) state of functionality at the time of the analysis, depending on the inherent degradation rate of the system as well as on the level of functional loss reached after the occurrence of the first disruption and the subsequent escalation scenarios. This affects the values of the transition rates within the Markov chain model represented in Fig. 3-a). Thus, for example, two different values for λ_1 shall be considered to account for high and low absorption abilities of the system.

In general, λ is associated with the failure process of a system, while μ reflects the repair process. In particular, λ_1 is calculated as the inverse of the *MTBF* (Mean Time Between Failure) of the system after disruptions, which is the time between the occurrence of the disruption and the system failure, and reflects the absorption ability of the system, while λ_2 is evaluated as the inverse of the *MTBF* of the system at normal conditions, which can be obtained from the analysis of operational records. Therefore, λ_2 is independent of the escalation scenarios considered. Differently, μ_1 and μ_2 reflect the adaptation and restoration abilities of the system. Specifically, μ_1 is derived as the inverse of the *MTTR* (Mean Time To Repair) associated with the self-response of the system to the external disturbance, while μ_2 is calculated as the inverse of the *MTTR* required by external maintenance to return the system to normal conditions or to a state in which the final outcomes of the disruption or escalation scenario are eliminated (e.g., fire is extinguished), even if other actions (e.g., repair of damaged equipment) are required to restore the system to normal operation. The *MTBF* and *MTTR* values are usually assessed by means of the statistical Maximum Likelihood Estimation (MLE) method [64].

The transition of the system functionality due to failure (e.g., the failure of the system after disruptions and the degradation of the system over time) and repair (e.g., the intervention of internal safety systems and the external intervention of firefighters) processes can be modeled by different types of Markov chains [63,65]. These provide the transition probabilities for the system to move from one state to another, capturing changes in functionality over time due to failure and response processes.

In particular, the adoption of a continuous-time Markov chain (CTMC) to model the failure of the system after external disturbances over time is consolidated [65,66], since it is reasonable to consider that the failure probability depends solely on the most recently known time step and not on the previous steps (memoryless property) [10]. Thus, the transition probabilities among the states associated with this process are described assuming an exponential model [66,67], as follows:

$$P_E(\lambda_1;t) = \int_{t_0}^{t} \lambda_1 e^{-\lambda_1 t} dt = 1 - e^{-\lambda_1 t} \tag{4}$$

where λ_1 represents the transition rate in disrupted conditions and t_0 denotes the time at which the disruption occurs.

On the contrary, the intervention of internal safety systems and the external intervention of firefighters are better modelled by non-homogenous continuous-time Markov chains (NHCTMCs) as the probability of intervention increases with time, reflecting the growing likelihood of response as the events progress [63]. Different probability distribution models can be used to describe the probabilities of

transitioning from one state to another for these processes [67,68], such as the Weibull distribution [69,70] or the normal / log-normal distribution [71,72].

For the sake of brevity, the model considered in the case study, i.e., a normal distribution modelling the MTTR, is reported below. The model is referred to both self-repair processes (as for μ_1) or external processes (as for μ_2):

$$P_N\left(\mu_{MTTR}, \delta^2_{MTTR};\ t\right) = \int_{-\infty}^{t} \frac{1}{\sqrt{2\pi\delta^2_{MTTR}}} e^{-\frac{(t-\mu_{MTTR})^2}{2\delta^2_{MTTR}}} dt = 0.5\left(1 + erf\left(\frac{t-\mu_{MTTR}}{\delta_{MTTR}\sqrt{2}}\right)\right) \quad (5)$$

where μ_{MTTR} and δ_{MTTR} represent the mean and the standard deviation of the *MTTR* distribution.

Clearly, the selection of the most appropriate distribution depends on the available data and/or prior experience [67]. NHCTMCs are suggested also for the modelling of the degradation of the system over time [63]. However, a simplified assumption entails considering a uniform distribution over time to calculate the reliability degradation rate [67], as follows:

$$P_C(\lambda_2) = C \quad (6)$$

where C is a value between 0 and 1 (0 denotes no degradation over time, 1 denotes maximum degradation over time).

Table 1 shows the transition probabilities for the N^{th} escalation scenario (*Block N* in Fig. 3-a)) based on the models and probability distributions reported in Eqs. (4)-(6).

2.3.4. DBN development in the event of escalation scenarios

In case of escalation scenarios, multiple DBNs (see Fig. 3-b)) are required to assess the system resilience by the metrics defined in Section 2.3.2. In particular, the number of required DBNs corresponds to the number of external disturbances encompassing the disruption event and the alternative escalation scenarios. This arises from the need to represent different scenarios occurring over time, along with changing the resilience attributes whenever a new scenario occurs. Therefore, extending to N escalation scenarios, each Markov chain associated with every block shown in Fig. 3-a) shall be converted into a DBN, as illustrated in Fig. 3-b). Details regarding the structure of the DBNs and the associated conditional probabilities are provided in Section 2.4.

2.4. Procedure for the quantitative assessment of resilience

Based on the conceptual framework and on the metric introduced in Section 2.3, a specific methodology has been developed for the quantitative assessment of the resilience of engineered systems in the case of escalation scenarios. The procedure consists of five subsequent steps, as shown in the flowchart reported in Fig. 4.

Step 1. involves collecting the necessary data to conduct the quantitative assessment of resilience (i.e., the input data required for the application of the methodology). In particular, this includes information concerning the layout of the engineered system under assessment, the substances involved, the operating conditions of the equipment units (i.e., pressure and temperature), the type and operation of the safety systems and safety barriers (SBs) implemented in the facility analyzed, as well as relevant information concerning maintenance, plant inspections, and other specific procedures.

Step 2. of the proposed methodology requires the identification of the accident paths that may affect the engineered system under assessment. This involves both the identification of the sequence of physical scenarios (the first disruption and the consequent escalation scenarios) that may occur, defining them within the timeline of events (i.e., definition of time intervals between the scenarios), and the identification of the specific preventive, controlling, and mitigative SBs, which may be involved in each accident path.

The accident path typically consists of three steps:

Table 1
Transition probabilities of the novel Markov chain model in the event of N escalation scenarios.

Transition rates	S1	S2	S3	S4	…	$S2_i$	$S3_i$	$S4_i$	…	$S2_N$	$S3_N$	$S4_N$
S1	$1 - P_E(\lambda_1^N, t)$	0	0	0	0	0	0	0	0	$P_E(\lambda_1^N, t)$	0	0
S2	0	$1 - P_E(\lambda_1^N, t)$	0	0	0	0	0	0	0	$P_E(\lambda_1^N, t)$	0	0
S3	0	0	$1 - P_E(\lambda_1^N, t)$	0	0	0	0	0	0	$P_E(\lambda_1^N, t)$	0	0
S4	0	0	0	$1 - P_E(\lambda_1^N, t)$	0	0	0	0	0	$P_E(\lambda_1^N, t)$	0	0
…	0	0	0	0	$1 - P_E(\lambda_1^N, t)$	0	0	0	0	$P_E(\lambda_1^N, t)$	0	0
$S2_i$	0	0	0	0	0	$1 - P_E(\lambda_1^N, t)$	0	0	0	$P_E(\lambda_1^N, t)$	0	0
$S3_i$	0	0	0	0	0	0	$1 - P_E(\lambda_1^N, t)$	0	0	$P_E(\lambda_1^N, t)$	0	0
$S4_i$	0	0	0	0	0	0	0	$1 - P_E(\lambda_1^N, t)$	0	$P_E(\lambda_1^N, t)$	0	0
…	0	0	0	0	0	0	0	0	$1 - P_E(\lambda_1^N, t)$	$P_E(\lambda_1^N, t)$	0	0
$S2_N$	0	0	0	0	0	0	0	0	0	$1 - P_N\left(\mu_{MTTR_1^N}, \delta^2_{MTTR^N};\ t\right)$	$P_N\left(\mu_{MTTR_1^N}, \delta^2_{MTTR^N};\ t\right)$	0
$S3_N$	0	0	0	0	0	0	0	0	0	0	$1 - P_N(\mu_{MTTR_2^N}, \delta^2_{MTTR^N};\ t)$	$P_N\left(\mu_{MTTR_2^N}, \delta^2_{MTTR^N};\ t\right)$
$S4_N$	$P_C(\lambda_2)$	0	0	0	0	0	0	0	0	0	0	$1 - P_C(\lambda_2)$

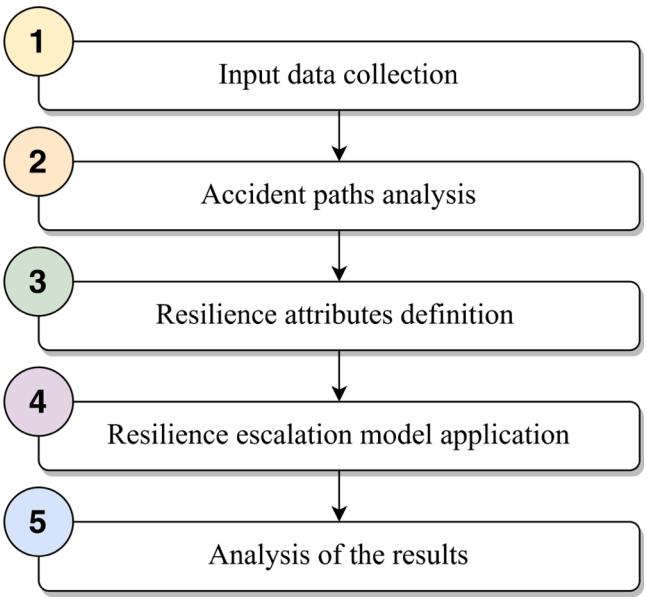

Fig. 4. Flowchart of the methodology proposed in the current study for the quantitative assessment of resilience in the event of escalation scenarios.

1. Initiation, which consists in the disruption event where an accident starts;
2. Propagation, entailing the sequence of events that maintain or expand the initial accident;
3. Termination, encompassing the events or actions aimed at resolving the accidental event.

Identifying the first disruption event (initiation) requires performing hazard identification and analysis. Since the goal is to identify process-related major hazards (i.e., hazards leading to releases of materials and/or energy), the conventional HAZard and OPerability (HAZOP) study [73] can be used for this purpose.

The accident scenarios following the initiating event must then be identified (propagation). In this regard, the failure analysis of the SBs in place aimed at preventing, controlling, and mitigating the secondary accidents is crucial for conducting a comprehensive accident path analysis. Therefore, suggested methods to carry out this task are the Bow-Tie Analysis [68] or the systematic System Hazard Identification, Prediction and Prevention (SHIPP) methodology [61]. However, it is important to remark that these methods do not address the possibility of accident propagation involving secondary equipment (domino effect). Thus, additional approaches shall be applied to complement the analysis and obtain a comprehensive overview of the entire accident propagation path. The relevant literature concerning the quantitative assessment of domino effect in chemical, process, and Oil&Gas industries [18,19,62] provides several methodologies aimed at the specific analysis of propagation possibility and probability, to which the reader is referred for details.

Finally, termination is the stage in which tailored restoration attempts are carried out to repair damages and resolve the reduction in system functionality. Interventions aimed at solving the escalation scenario or repairing the engineered system through inspections, maintenance and, eventually, equipment replacement, are examples of common practices. Emergency and rescue plans should also be considered for a comprehensive analysis of the restoration operations.

Step 3. consists in the definition and quantification (in terms of occurrence probability) of the resilience attributes (absorption, adaptation, restoration, and learning) associated with each event included in the accident paths identified in Step 2 (i.e., first disruption event and subsequent escalation scenarios). Except for learning, these attributes vary, based on the safety barrier activated in response to specific accidental events within the process accident sequence.

More specifically, absorption pertains to the inherent ability of the system to sustain or withstand external disruptions. Consequently, preventive measures and actions affect the absorption ability. Examples of preventive barriers include insulation materials, which aim to reduce damage to the equipment caused by heat or extremely low temperatures. Adaptation instead refers to the ability of the system to recover to the normal operational state without relying on external restoration actions. This attribute is characterized by inherent flexibility in self-responding to accidental situations and protection barriers, such as detection measures. For example, the emergency shut-down (ESD) system is a standard protection measure available in most industrial systems. Lastly, restoration, involving external contributions that return the system to the normal operational state, is represented by mitigative barriers and equipment maintenance and replacement. An example of restoration measures includes the intervention of firefighters in the event of a fire. Human reliability also influences restoration and consists of human effectiveness and involvement in disruption handling (e.g., operator level of training in inspection operations).

In order to determine and quantify the resilience attributes, fault tree analysis (FTA) can be employed [53]. Indeed, FTA enables the definition of resilience attributes through the generation of specific FTs which emphasize the causal relationships among root causes (also referred to as basic events (BEs)), leading to the failure or success of the safety barriers to which they are associated. It is worth noting that, depending on the system analyzed, there is the possibility of overlapping resilience attributes (i.e., safety barriers) between the different accidental events that may take place within the accident paths under consideration. The quantification of FTs and, consequently, of the resilience attributes, requires the identification of specific occurrence probabilities of failure or success of the BEs. In this regard, generic literature sources [7,14,55,74] can be consulted, alongside more specialized technical databases such OREDA [75]. FTs shall not be applied to the learning attribute, since it can occur or not depending on the availability of past experience.

In Step 4. the resilience escalation model proposed in Section 2.3 shall be applied to each accident path identified in Step 2. More in detail, given an accident path, for each event (i.e., the first disruption and the subsequent escalation scenarios) a specific DBN shall be generated. All the DBNs are expected to adhere to the generic structure shown in Fig. 5, which represents a simplified framework for measuring variations in system functionality states [10]. Thus, the general structure represented in the figure shall be applied to generate the specific DBN. The generation of the DBN is typically carried out by the application of tools for the development and deployment of decision support systems aimed at reasoning and decision making under uncertainty. Two notable software packages supporting the definition of DBNs are Hugin [76] and GeNIe Modeler [77], both relying on BNs and influence diagram tools.

As shown in Fig. 5, the specific framework comprises six main nodes ("*First disruption / Escalation scenario*", "*State of functionality*", "*Absorption*", "*Adaptation*", "*Restoration*", and "*Learning*") plus nodes "*Contributing element*" associated with the resilience attributes (in dashed line as their arrangement cannot be determined *a priori* but shall be tailored to the specific cases). The nodes "*First Disruption / Escalation scenario*", "*Learning*" and part of the nodes "*Contributing element*" constitute the root nodes of the DBN, while the node "*State of functionality*" is the leaf node. These nodes "*Contributing element*" correspond to the BEs identified through the FTA. The resilience attribute nodes "*Absorption*", "*Adaptation*", and "*Restoration*" alongside the rest of the nodes "*Contributing element*", instead, are intermediate nodes. The arcs (arrows) of the DBN denote the relationships among the nodes. Thus, the change in system functionality is a collective result of the disruption/escalation scenario in the current state, the resilience attributes at current states, and the system functionality at its previous states (previous

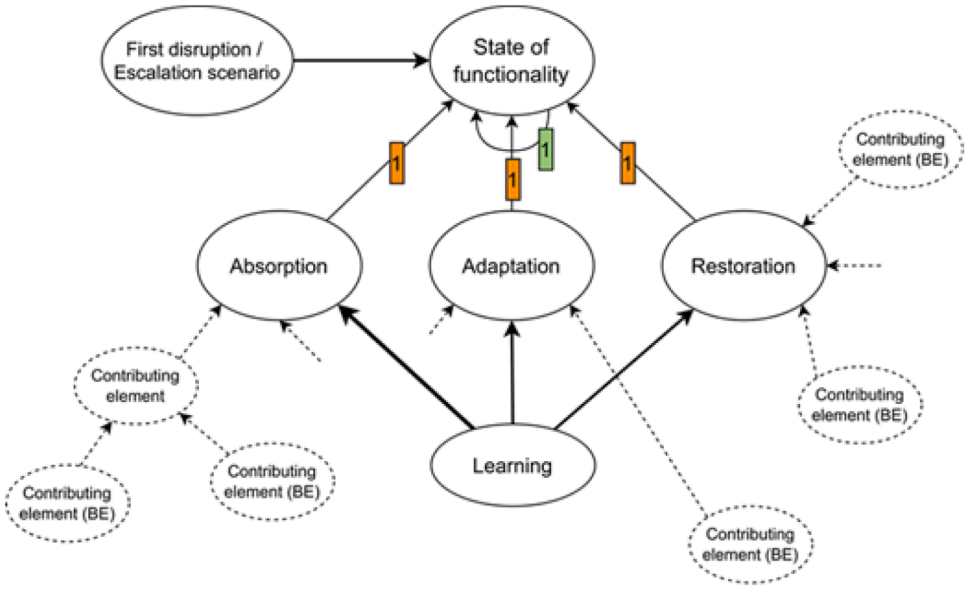

Fig. 5. The simplified general DBN structure assumed to measure the variations in system functionality states (BE, basic event) [10].

time steps). In the absence of external disturbances, the state of functionality of the system is conditionally dependent on its prior states (indicating a natural time-dependent degradation process of the system). In the DBN, all the time-dependent nodes involve temporal influences of the first order (i.e., influences between neighbouring time steps). More details regarding the order of the arcs are reported elsewhere [10,78].

After constructing the DBNs, it is necessary to define the states of each node. In general, the nodes assume two states, except for the node "*State of functionality*", which is characterized by four or more states depending on whether the system it is solely affected by the first disruption event or also by escalation scenarios (see Section 2.3.3 and Fig. 3-a), where the Markov chain is outlined). The node "*First disruption / Escalation scenario*", which reflects the occurrence of accidental events at any time during the operation process, can be in the state of YES (or NO) depending on whether the disruption or escalation scenario in question occurs (or does not occur). The same logic applies to the node "*Learning*", which is based on the presence or absence of past experience. The states of nodes "*Absorption*", "*Adaptation*", and "*Restoration*", instead, can be set as HIGH or LOW, depending on the effectiveness of their performance in carrying out their pre-established tasks at the time of the analysis. Finally, the nodes "*Contributing element*" can be in either a state of SUCCESS (S) or FAILURE (F), depending on the state of the BE under investigation for the part of root nodes, or based on the results of FTA (Boolean logic) for the part of non-root nodes.

Once the DBNs have been created and detailed, they must be quantified through the fulfillment of Conditional Probability Tables (CPTs) for each node present in each DBN. Those associated with the root nodes involve marginal probabilities, while the ones linked to the non-root nodes (i.e., intermediate and leaf nodes) concern conditional probabilities.

More in detail, for the node "*State of Functionality*", two distinct CPTs are required:

1. *First CPT*. This CPT defines the state of the node "*State of Functionality*" at the occurrence of the related disruption event or escalation events (initial conditions). In the case of the first disruption event, the system is assumed to be in state $S1$ at the start of system operations. Differently, in the case of escalation scenarios, this CPT reflects the functionality state based on the values from the time step immediately preceding the unfolding of the escalation scenario.
2. *Second CPT*. This second CPT represents the probability of state transitions at subsequent time steps and is crucial to define how functionality evolves over time (evolving conditions). Unlike the first CPT, this second CPT is independent of specific accidental events (whether they are initial disruptions or escalation scenarios). Instead, it is determined by the transition probabilities from the Markov chains, reflecting how likely it is for the system to move from one state to another (refer to Table 1 in Section 2.3.3).

By doing so, the Markov chain underpins the transition probabilities for the node "*State of Functionality*" across time steps, capturing the likelihood of shifts in system functionality regardless of the first disruption or escalation scenarios.

In contrast, for all the other time-independent nodes, a single CPT must be assigned. The CPT of the root node "*First disruption / Escalation scenario*" shall be compiled with the marginal probability of occurrence of the accidental scenario under consideration. Typically, a unit probability of occurrence is assigned to the state YES, aiming to analyse the system after the initial accident event has occurred. The same approach applies to node "*Learning*", whose CPT is influenced by the presence or absence of past experience. Setting the state of node "*Learning*" to YES, equal to 1, indicates available past experience with the same engineered system, while setting it to 0 implies a lack of past experience. Alternatively, setting it to a value higher than 0 and lower than 1 implies that data is available concerning similar equipment, with the specific value being determined by the amount of available data and the similarity of the system.

Then, the CPTs of the root nodes "*Contributing element*" (i.e., the BEs) are defined by marginal probabilities of success or failure, retrieved as discussed in Step 3, while the CPTs of the non-root nodes "*Contributing element*" adhere to the Boolean logic resembling "AND" and "OR" gates in FTs. Rules for CPTs deriving from FTAs are reported elsewhere in [55, 74].

Lastly, the CPTs of nodes "*Absorption*", "*Adaptation*", and "*Restoration*" are constructed considering all their parent nodes contributing equally to the probability of HIGH (H) or LOW (L) performance of the resilience attributes. In order to better understand these rules, three different examples of CPTs involving two, three, or four parent nodes (i.e., nodes "*Contributing element*" (CE)) are reported in the following in Table 2.

After the quantification of the CPTs, DBNs must be sequentially computed following the timeline of events of the accident path

Table 2
Rules for CPTs associated with two, three or four nodes labelled as "*Contributing elements*" (CE) entering an intermediate node characterized by two possible states: HIGH (H) and LOW (L). S, Successful; F, Failure.

CE	**S**		**F**												
CE	**S**	F	S	F											
H	1	0.5	0.5	0											
L	0	0.5	0.5	1											
CE	**S**				**F**										
CE	**S**		**F**		**S**		**F**								
CE	**S**	**F**	**S**	**F**	**S**	**F**	**S**	**F**							
H	1	0.67	0.67	0.33	0.67	0.33	0.33	0							
L	0	0.33	0.33	0.67	0.33	0.67	0.67	1							
CE	**S**								**F**						
CE	**S**				**F**				**S**		**F**		**F**		
CE	**S**		**F**		**S**		**F**		**S**		**S**		**S**		**F**
CE	**S**	**F**	**S**	**F**	**S**	**F**	**S**	**F**	**S**	**F**	**S**	**F**	**S**	**F**	**S**	**F**
H	1	0.75	0.75	0.5	0.75	0.5	0.5	0.25	0.75	0.5	0.5	0.25	0.5	0.25	0.25	0
L	0	0.25	0.25	0.5	0.25	0.5	0.5	0.75	0.25	0.5	0.5	0.75	0.5	0.75	0.75	1

identified in Step 2. By doing so, the state of functionality curves associated with each accidental event (disruption event and subsequent escalation scenarios) of each accident path are obtained. In order to generate the resilience curves, the same tools mentioned for the construction of the DBNs' frameworks can be used, i.e., Hugin [76] and GeNIe Modeler [77].

Then, in order to develop the resilience curve, Eq. (3) (Section 2.3.2) must be applied. It is essential to remind that in order to obtain the overall resilience curve of the system for a given accident path, it is necessary to combine the values of the state of functionality from the different computed DBNs within their respective validity time ranges in the path timeline (defined in Step 2 by the time intervals between the accidental events in the accident paths) [10].

Lastly, in Step 5. the results obtained shall be analyzed and discussed. The focus is mainly dedicated to the examination of the developed resilience curves (e.g., time required to restore a high functionality of the system, identification of potential design improvements, etc.). However, Step 5 also provides the opportunity to discuss and apply further investigations based on the scope of the study. For instance, "posterior analysis" within the context of Bayesian network can be employed to observe how the system restores in the face of continuous solicitations or threats posed by specific elements. This analysis may involve assuming specific failure causes as evidence and analyzing their impact on the resilience of the system. Additionally, sensitivity analysis can be performed to assess the impact of changes in failure and repair rates on the resilience curves.

3. Case study

The transfer of cryogenic fuels, such as LNG or LH_2, from shore-based storage facilities to the onboard tanks of ships is known as cryogenic bunkering. There are three primary bunkering configurations, namely truck-to-ship (TTS), land-to-ship (LTS), and ship-to-ship (STS), each of which fulfills specific logistical and infrastructural requirements [79]. While the LTS bunkering arrangement involves filling the onboard tanks of the cryogenic vessel directly from a stationary storage facility or liquefaction plant located at the port, the TTS bunkering configuration uses specially designed trucks equipped with cryogenic tanks to transport and deliver the fuel directly to the receiving vessel. As an alternative, the STS configuration is distinguished by a receiving vessel that serves as a mobile fuel station and is moored to the bunker vessel [80]. This final arrangement, which is schematized in Fig. 6, is the one considered as case study to demonstrate the application of the proposed methodology.

The transfer of LH_2, stored at extremely low temperature of about −253 °C, has been considered in the case study. Three different transfer lines can be identified in the scheme shown in Fig. 6: the LH_2 transfer line, for the transfer of the cryogenic substance, the Boil-Off-Gas (BOG) transfer line, to handle the gaseous hydrogen generated due to the heat exchange with the external environment that causes a partial vaporization of LH_2, and the helium (He) line, that is necessary to carry out sweeping operations before/after the transfer. The fuel is assumed to be transferred from the "bunker supply" to the "receiving vessel" via the use of a submerged cryogenic pump [81]. However, when the pressure differential is sufficient to guarantee a successful transfer, the pump may

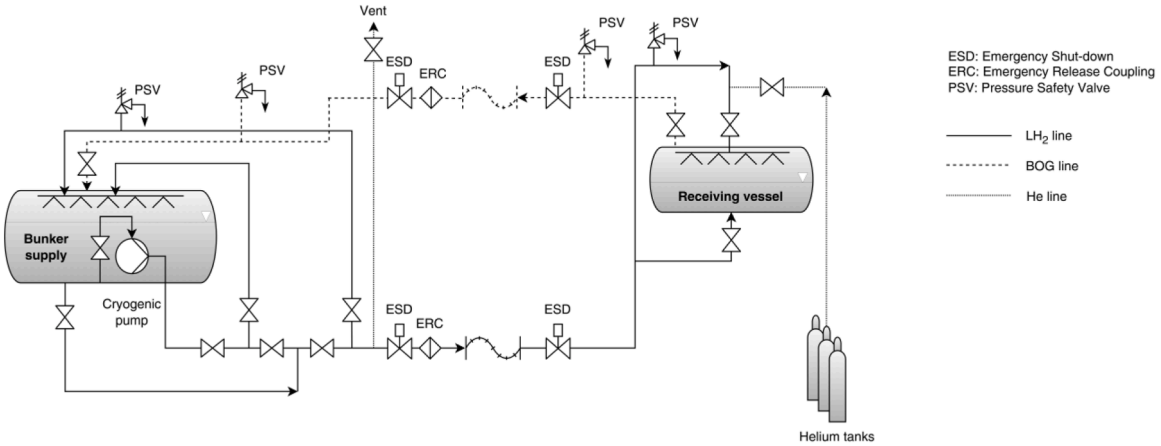

Fig. 6. Ship-to-ship bunkering scheme.

be stopped. The tanks are double-walled vacuum insulated through the adoption of aluminum-based multi-layer insulation (MLI). Furthermore, the transfer is carried out via a flexible hose. The hose protection system consists of a hydraulically operated Quick Connect Disconnect Coupler (QCDC), together with upper and lower Emergency Shut-Down (ESD) systems and an Emergency Release Coupling (ERC, which serves as a breakpoint within the LH_2 hose transfer system and is designed to minimize risk). Pressure Safety Valves (PSVs) are located on different lines to safeguard the equipment from pressurization and potential process safety incidents. Sequential filling is carried out to better control the pressure in the receiving tank. Starting with top filling (shower/-spray) is a common procedure to lower the pressure of the receiving tank. After a satisfactory pressure is reached, supply is switched to bottom filling. The BOG line allows excess vapor to return to the bunker supply cargo tank. Its adoption is not always necessary, especially for smaller transfers, but in the current case study it is considered since it contributes to the reduction of transfer times. In general, the pressure regulating capability of the receiving tank determines whether a BOG line is required or not [82].

4. Results

In the following, the results of the application of the proposed methodology to the case study considered are shown.

In Step 1 (see Fig. 4), input data were collected. They include the system layout, substance properties (thermodynamic, physical, and hazard), technical procedures (e.g., ordinary bunkering operations, inspection and maintenance, and so on), and safety devices (see Section 3).

In Step 2 (see Fig. 4), the SHIPP methodology [61] was used to identify and characterize the accident sequential paths of the first disruption event resulting from hazardous conditions affecting the bunkering area analyzed. Then, the procedure suggested by Cozzani et al. [17] was applied to determine the potential escalation scenarios.

More in detail, the occurrence of events such as malfunctions of the BOG removal system, falling objects, natural adverse conditions, malicious interventions, and so on, have been identified as the possible causes of minor leakages of LH_2 from the flexible hose connecting the bunker supply and the receiving vessel. The accident propagation path may then involve a wide range of possible scenarios. If the release occurs on the water surface, it may trigger the Rapid Phase Transition (RPT) phenomenon, which is a violent physical explosion caused by the interaction between liquids with significantly differing temperatures and boiling points [79]. On the contrary, immediate or delayed ignition of the evaporated hydrogen gaseous cloud could occur [83]. Recent full-scale experimental campaigns have shown that no RPTs occurred following LH_2 spills onto water [84–86]. Although these results do not entirely exclude the possibility of RPT, its likelihood can be considered low based on available experimental evidence. As a result, the scenario was not further considered [87].

On the other hand, the possibility of ignition in the case of atmospheric releases of LH_2 is highly probable due to the wide flammability range and low ignition energy of hydrogen [79]. In particular, immediate ignition was identified as the most frequently observed outcome, as noted by sources such as the Safe Hydrogen Fuel Handling and Use for Efficient Implementation (SH_2IFT) project [84]. Consequently, a jet-fire resulting from a minor LH_2 release emerges as the most probable scenario [83].

Such a scenario raises significant safety concerns and has the potential to trigger domino effects involving the adjacent equipment, including the bunkering system. Indeed, in the event of a jet-fire impinging the onboard hydrogen vessels, the potential for a Boiling Liquid Expanding Vapor Explosion (BLEVE) associated to a fireball arises as the most probable scenario, amplifying the risks to personnel, assets, and the environment [88].

Given the results obtained by the application of the SHIPP methodology and domino effect literature, and considering that release and immediate ignition can be considered as two simultaneous events, the following scenarios were taken into account for the quantitative assessment of resilience of the bunkering system under analysis:

1. A minor LH_2 release with immediate ignition (jet-fire), deemed as the first disruption event occurring at the start of system operation;
2. A BLEVE associated with a fireball following jet-fire impingement upon hydrogen tanks, considered as the escalation scenario occurring after 30 min (time to failure (TTF)).

It is important to underline that a TTF of 30 min aligns with the insulation material of the tank considered in the case study (i.e., aluminum-based MLI) as reported in [89]. However, different values shall be considered for other insulation materials. The latter can be estimated using specific models, such as those proposed in [90].

Fig. 7 reports the process accident model associated with the minor release of LH_2 considered in the case study, along with the six safety barriers identified and selected for the system: the Release Prevention Barriers (RPBs), the Release Detection Barriers (RDBs), the Ignition Prevention Barriers (IPBs), the Escalation Prevention Barriers (EPBs), the Human Factor Barriers (HFBs), and the Management & Organizational Barriers (M&OBs) [61]. These last two non-technical SBs affect all the other ones, as indicated in Fig. 7.

In Step 3 (see Fig. 4), the resilience attributes for each scenario were defined. As suggested in the description of the proposed methodology, this information was obtained by the application of FTA to the safety barriers involved in the system analyzed (i.e., RPBs, RDBs, IPBs, and EPBs, see Fig. 7). The FTs generated are shown in Figs. A.1-A.4 in the Appendix. It is noteworthy that no dedicated FTs were created for HFBs and M&OBs, as human and organizational factors influence all the other SBs and the possible failures can be directly incorporated into the FTs developed for the other SBs.

The absorption attribute can be defined though the FTs associated with part of the RPBs and the IPBs, since they reflect the preventive measures of the system (e.g., corrosion protection, overpressure protection, sparks inhibitor protection, etc.), while the adaptation attribute can be defined through part of the FTs related to the RDBs and the EPBs. Indeed, adaptation reflects the mitigative barriers of the system associated with the detection of the release (e.g., hydrogen release detection) and the mitigation of escalation phenomena (e.g., smoke and flame detection). The restoration attribute has the same role of the adaptation attribute but is approached from an external intervention perspective. This explains why its contributing elements cannot be defined through the FT analysis applied to the SBs of the system. Furthermore, the restoration attribute is site-specific, thus an in-depth knowledge of the system under investigation is necessary to determine its contributing elements.

A graphical representation of the resilience attributes, together with the DBN obtained in Step 4 of the procedure, is shown in Fig. 8 for the first disruption and in Fig. 9 for the escalation scenario identified in Step 2. In the figures, absorption contributing elements are indicated in pink, adaptation contributing elements in blue and restoration contributing elements in orange. Different shades of colours are considered within the different groups of contributing elements. Marked colours represent the root causes of the resilience attribute trees, whereas muted colours represent the intermediate nodes leading to the top event intended as reduced performance of the resilience attributes. Actually, the FT analysis of the SB systems enables the identification of sequences of events that, starting from the root causes, culminate in the top event intended as the failure of the safety barrier itself.

Once resilience attributes are defined, they shall be quantified. Table 3 reports the occurrence probabilities assigned to the BEs of the resilience attributes.

The values were retrieved from specific literature sources [7,14,38,55,61,91], from the OREDA database [75], and applying Human Reliability Analysis (HRA) [92]. More specifically, technical literature

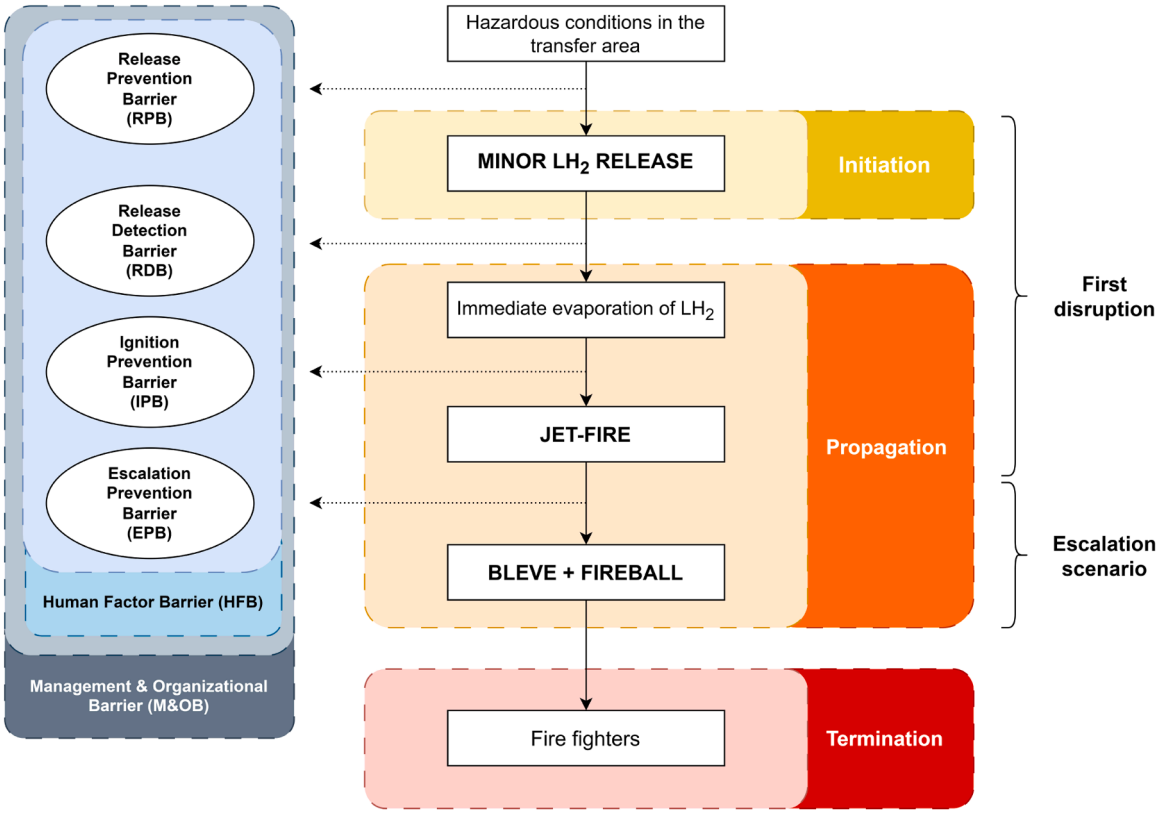

Fig. 7. The process accident model developed for the considered case study.

sources were adopted to determine the occurrence probability of technological, organizational, and managerial BEs, while HRA was considered to ascertain the probability of occurrence of human impact factors. The Standardized Plant Analysis Risk-HRA (SPAR-H) method was selected and three Performance Shaping Factors (PSFs): stress, training, and procedures were derived to calculate the Human Error Probability (HEP) [93]. When looking at the table, it should be remarked that the event labelled as "Vacuum PSV fails to open" has been assigned a specific occurrence probability, lower than that of PSV failure.

Among the root nodes, the one labeled "*Emergency maintenance*" stands out as the only node not included in the FTs. This omission is due to its involvement in the restoration process as external action. A failure probability of 0.04 was assigned to it, based on recommendations from literature reports [55].

In Step 4 (see Fig. 4), the DBNs were constructed for each accidental event in the accident path selected in Step 2, quantified and lastly computed using GeNIe Modeler [77].

As mentioned above, the DBN obtained for the first disruption event (minor LH_2 release with immediate ignition) is reported in Fig. 8, while that for the escalation scenario (BLEVE and fireball following jet-fire impingement on secondary equipment) is displayed in Fig. 9.

The node "*First disruption / Escalation scenario*" is characterized by states YES = 1 and NO = 0, indicating that both the first disruption (Fig. 8) and the escalation scenario (Fig. 9) certainly occurred. The same logic applies to node "*Learning*", which is characterized by states YES = 1 and NO = 0 in both the DBNs, indicating that past experience concerning the same system aids in improving future system recovery. The remaining root nodes of the two DBNs, resembling the root nodes "*Contributing element*", are compiled with the marginal probabilities of the BEs acquired in the previous step (see Table 3). On the contrary, the non-root nodes "*Contributing element*" are characterized by CPTs obtained from the application of the Boolean "AND" and "OR" gates of the FT illustrated in Appendix (Figs. A.1-A.4).

The intermediate nodes "*Absorption*", "*Adaptation*", and "*Restoration*" in both the DBNs are instead characterized by states HIGH (H) and LOW (L), depending on the effectiveness of the safety barriers, i.e., of the performance of the resilience attributes resulting from the application of the FTA mentioned in Step 3. The CPTs associated with these resilience attributes were specified considering an equal distribution of the occurrence probability of the parent nodes as already described in Section 2.4.

Lastly, according to the resilience model proposed in the present study (see Section 2.3.1), the node "*State of functionality*" of DBN in Fig. 8 has four states, named $S1$, $S2$, $S3$, and $S4$, while the DBN in Fig. 9 has seven states, named $S1$, $S2$, $S3$, $S4$, $S2_1$, $S3_1$, and $S4_1$. The CPTs (see Section 2.4) of node "*State of Functionality*" are quantified based on the Markov chain rules described in Section 2.3.3, assuming the transition rates outlined in Table 4 and Table 5. It is noteworthy that different transition rates (H and L) were assumed based on the state of the system: i.e., its degradation rate at the analysis time.

In order to recall, an exponential distribution was considered to describe the transitions associated with the failure rates λ_1 and λ_1^1, a normal distribution was applied to define the transitions linked to the repair rates μ_1, μ_2, μ_1^1, and μ_2^1, and a constant distribution for the reliability degradation process associated with λ_2. In the case of the normal distribution, a standard deviation value (δ) of 30 % with respect to the average value was considered, as suggested by [94].

For the sake of brevity, only the CPTs of the node "*State of functionality*" associated with the DBN in Fig. 8 (first disruption) are reported below in Table 6 (for the initial time step, $t = 0$) and Table 7 (for the subsequent time steps, $t \geq 1$), based on the values of Table 4 and the Markovian rules presented in Table 1.

The two quantified DBNs were then computed for two different durations, assuming that each time step of the simulations represents one minute of operation. The first DBN (Fig. 8) considered 30 min of operation, since this is the typical time after which the aluminum-based MLI considered for the hydrogen tanks fails due to the external heat caused

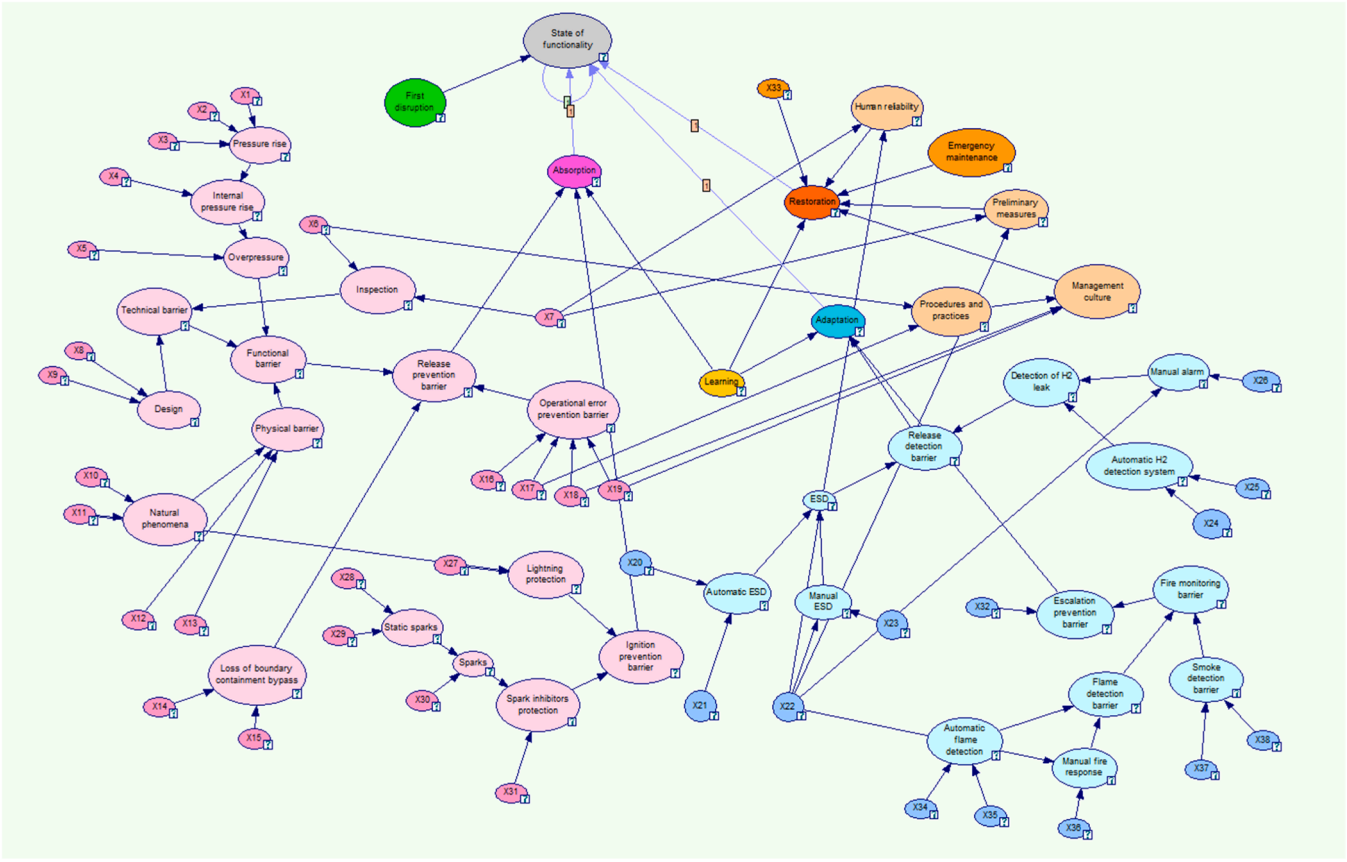

Fig. 8. The DBN model associated with the first disruption (minor LH_2 release with immediate ignition) of the considered case study. Obtained with GeNIe Modeler [75].

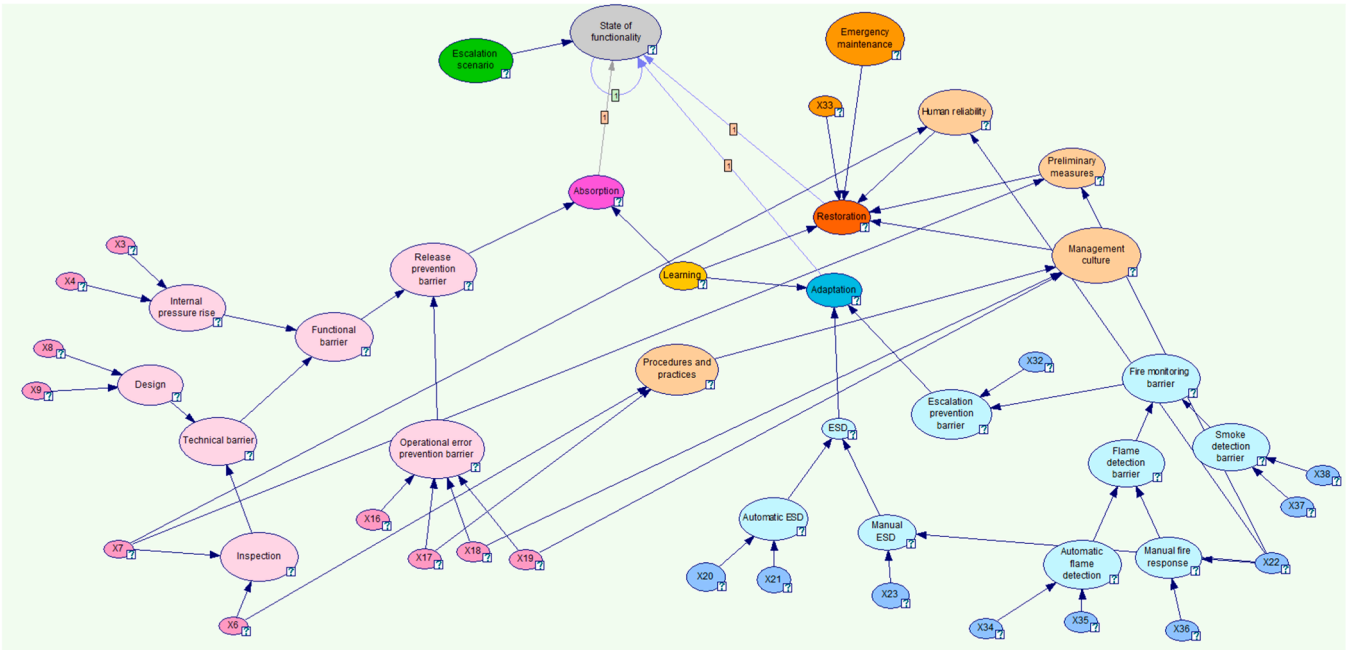

Fig. 9. The DBN model associated with the escalation scenario (BLEVE and fireball following jet-fire impingement on secondary equipment) of the considered case study. Obtained with GeNIe Modeler [77].

by the jet-fire [89]. The second DBN (Fig. 9) is simulated until the functionality of the system is restored to 1. In the analysis of the case study, the intention of achieving full recovery following replacement interventions was not considered. Actually, since the resilience model was applied to major accident scenarios rather than to process operability-related incidents (e.g., production outage due to system

Table 3
Failure probabilities of the basic events (BEs) considered in the examined case study.

Code	BEs description	Occurrence probability
X1	Inadequate purging	4.77×10^{-2}
X2	BOG removal malfunction	4.10×10^{-5}
X3	External fire	1.54×10^{-4}
X4	Vacuum PSV fails to open	2.12×10^{-5}
X5	Pressure shock in hose	4.77×10^{-2}
X6	Inadequate inspection and testing procedures	2.00×10^{-2}
X7	Error in manual inspection	9.82×10^{-3}
X8	Defects	1.44×10^{-2}
X9	Corrosion	2.00×10^{-3}
X10	Adverse weather conditions	1.14×10^{-1}
X11	Lighting	3.40×10^{-2}
X12	Dropped objects	2.80×10^{-3}
X13	Malfunction intervention	2.80×10^{-4}
X14	Valve left open	4.77×10^{-2}
X15	Valve opened during operation	4.77×10^{-2}
X16	Inadequate control system	5.00×10^{-2}
X17	Inadequate maintenance procedures	5.00×10^{-2}
X18	Inadequate supervision	3.40×10^{-2}
X19	Inadequate training	2.50×10^{-2}
X20	ESD sensors failure	2.74×10^{-1}
X21	Automatic ESD valves failure	1.17×10^{-1}
X22	Delay in manual operation	4.77×10^{-2}
X23	Manual ESD valves failure	2.11×10^{-2}
X24	Hydrogen sensors failure	7.54×10^{-3}
X25	Hydrogen alarm failure	2.52×10^{-3}
X26	Pressure gauge failure	1.54×10^{-4}
X27	Lightning protection issues	3.94×10^{-3}
X28	Static sparks from operators	1.25×10^{-1}
X29	Static sparks from equipment	3.31×10^{-3}
X30	Electrical sparks	3.06×10^{-3}
X31	Spark inhibitors protection issues	4.00×10^{-2}
X32	Fire suppression system failure	5.58×10^{-2}
X33	Firefighting actions failure	9.02×10^{-2}
X34	Flame alarm failure	2.10×10^{-2}
X35	Automatic ignition source detection failure	2.53×10^{-1}
X36	Manual fire alarm failure	5.00×10^{-2}
X37	Smoke alarm failure	2.10×10^{-2}
X38	Smoke detection sensors failure	7.41×10^{-2}

Table 4
Transition rates of functionality associated with the first disruption.

Transition rates	Unit	H	L
λ_1	min^{-1}	0.1	0.125
μ_1	min^{-1}	0.5	0
μ_2	min^{-1}	0.017	0
λ_2	min^{-1}	0.001	0.001

Table 5
Transition rates of functionality associated with the escalation scenario.

Transition rates	Unit	H	L
λ_1^1	min^{-1}	2	3.03
μ_1^1	min^{-1}	0.1	0
μ_2^1	min^{-1}	0.006	0
λ_2	min^{-1}	0.001	0.001

Table 6
CPT of the node "*State of functionality*" of the DBN in Fig. 8 at $t = 0$.

First disruption	YES	NO
*S*1	1	1
*S*2	0	0
*S*3	0	0
*S*4	0	0

Table 7
CPT of the node "*State of functionality*" of the DBN in Fig. 8 at $t \geq 1$.

First disruption	**YES**																															
State of the system [t-1]	***S*1**								***S*2**								***S*3**								***S*4**							
Absorption [t-1]	**H**				**L**				**H**				**L**				**H**				**L**				**H**				**L**			
Adaptation [t-1]	**H**		**L**		**H**				**H**		**L**		**H**		**L**		**H**		**L**		**H**		**L**		**H**		**L**		**H**		**L**	
Restoration [t-1]	**H**	**L**	**H**	**L**	**H**	**L**	**H**	**L**	**H**	**L**	**H**	**L**	**H**	**L**	**H**	**L**	**H**	**L**	**H**	**L**	**H**	**L**	**H**	**L**	**H**	**L**	**H**	**L**	**H**	**L**	**H**	**L**
***S*1**	0.9	0.9	0.9	0.9	0.88	0.88	0.88	0.88	0	0	0	0	0	0	0	0	0	0	0	0	0	0	0	0	0.01	0.01	0.01	0.01	0.01	0.01	0.01	0.01
***S*2**	1	1	1	1	0.12	0.12	0.12	0.12	0.95	0.95	1	1	0.95	0.95	1	1	0	0	0	0	0	0	0	0	0	0	0	0	0	0	0	0
***S*3**	0	0	0	0	0	0	0	0	0.05	0.05	0	0	0.05	0.05	0	0	0.99	1	0.99	1	0.99	1	0.99	1	0	0	0	0	0	0	0	0
***S*4**	0	0	0	0	0	0	0	0	0	0	0	0	0	0	0	0	0.01	0	0.01	0	0.01	0	0.01	0	0.99	0.99	0.99	0.99	0.99	0.99	0.99	0.99
First disruption	**NO**																															
State of the system [t-1]	***S*1**								***S*2**								***S*3**								***S*4**							
Absorption [t-1]	**H**				**L**				**H**				**L**				**H**				**L**				**H**				**L**			
Adaptation [t-1]	**H**		**L**		**H**		**L**		**H**		**L**		**H**		**L**		**H**		**L**		**H**		**L**		**H**		**L**		**H**		**L**	
Restoration [t-1]	**H**	**L**	**H**	**L**	**H**	**L**	**H**	**L**	**H**	**L**	**H**	**L**	**H**	**L**	**H**	**L**	**H**	**L**	**H**	**L**	**H**	**L**	**H**	**L**	**H**	**L**	**H**	**L**	**H**	**L**	**H**	**L**
***S*1**	1	1	1	1	1	1	1	1	1	1	1	1	1	1	1	1	1	1	1	1	1	1	1	1	1	1	1	1	1	1	1	1
***S*2**	0	0	0	0	0	0	0	0	0	0	0	0	0	0	0	0	0	0	0	0	0	0	0	0	0	0	0	0	0	0	0	0
***S*3**	0	0	0	0	0	0	0	0	0	0	0	0	0	0	0	0	0	0	0	0	0	0	0	0	0	0	0	0	0	0	0	0
***S*4**	0	0	0	0	0	0	0	0	0	0	0	0	0	0	0	0	0	0	0	0	0	0	0	0	0	0	0	0	0	0	0	0

unavailability), the main focus is on mitigating the accidental events preventing more severe consequences (i.e., extinguishing the jet-fire and mitigating the fireball respectively): therefore, repair and/or replacement processes are not assessed in the case study. It should also be remarked that repair/replacement timelines may also span months, making this type of analysis beyond the scope of the current application. The GeNIe Modeler software [77] was used to analyze the DBNs within the specified time intervals. The output of the simulations, reported in Fig. 10-a), shows the states of system functionality considered in the case study. The dynamic resilience curve was then derived, based on Eq. (6), by adding the initial state ($S1$) of the system functionality and the final recovered functionality states of the system ($S4$ and $S4_1$), following the timeline of the two accidental events. The curve obtained is shown in Fig. 10-b).

The results of Step 5, in which the analysis of the findings is carried out, are included in the discussion section that follows.

5. Discussion

The present study proposes a systematic quantitative procedure based on Dynamic Bayesian Networks to assess the resilience of engineered systems in case of escalation scenarios (domino effect) by a dynamic (time-dependent) and probabilistic approach. Given the increasing interest in the concept of the domino effect in the chemical and process industry, as well as in the Oil&Gas facilities, the proposed resilience escalation model represents a pivotal tool for the investigation of the functionality of systems following subsequent accidental events. This study fills gaps in the availability of systematic quantitative methods able to assess the resilience of engineered systems in the context of both well-established (e.g., refineries, petrochemical units, or chemical manufacturing complexes) and innovative infrastructure (e.g., cryogenic bunkering system). Furthermore, given the generic nature of the procedure, it can be customized and applied to a wider range of infrastructure (e.g., automotive infrastructure).

The application of the proposed method to the ship-to-ship LH_2 bunkering configuration considered in the illustrative case study demonstrated its ability in assessing resilience when cascading accident scenarios occur. Moreover, it proved the quality of the results addressing the identification of weaknesses, through the FTA applied to classify the resilience attributes, as well as in ensuring business continuity in industrial systems.

When considering the results of the specific case study carried out, Fig. 10-b) shows the calculated resilience curve of the bunkering system considered. Two sharp declines of the curve are depicted, representing the functionality decrease of the system following the first disruption (i.e., the minor LH_2 release with immediate ignition (jet-fire)) and the subsequent escalation scenario (i.e., the BLEVE and fireball following jet-fire impingement). The latter occurs when the first disruption is not adequately managed: in fact, once the jet-fire is detected, the adaptation and restoration abilities of the system attempt to recover and restore functionality over time. If these actions are successful after the first disruption, no subsequent events take place, and the dashed black line in the graph applies. The dashed line demonstrates a steady and uneventful recovery, returning to full resilience (intended as the jet-fire extinction and the system reconditioning) in approximately 55 min. Otherwise, if the jet-fire is not effectively handled, a potential chain of events (in the current case study, a BLEVE and fireball following hydrogen tank catastrophic rupture) can occur, leading to increased damage to the system and amplified recovery time (about 170 min), as indicated by the solid black line. A two-hour difference in recovery time is calculated between restoration up to $S4$ (if only the first disruption occurs) and $S4_1$ (if the first disruption and the escalation scenario occur). An even higher time difference is expected in the case of equipment repair and/or replacement are addressed in the analysis, meaning that the system returns to a high functionality state (full recovery, state $S1$). In fact, while recovery from the first disruption (minor LH_2 release with immediate ignition) requires only repair, recovery from the escalation scenario (BLEVE and fireball following jet-fire impingement on

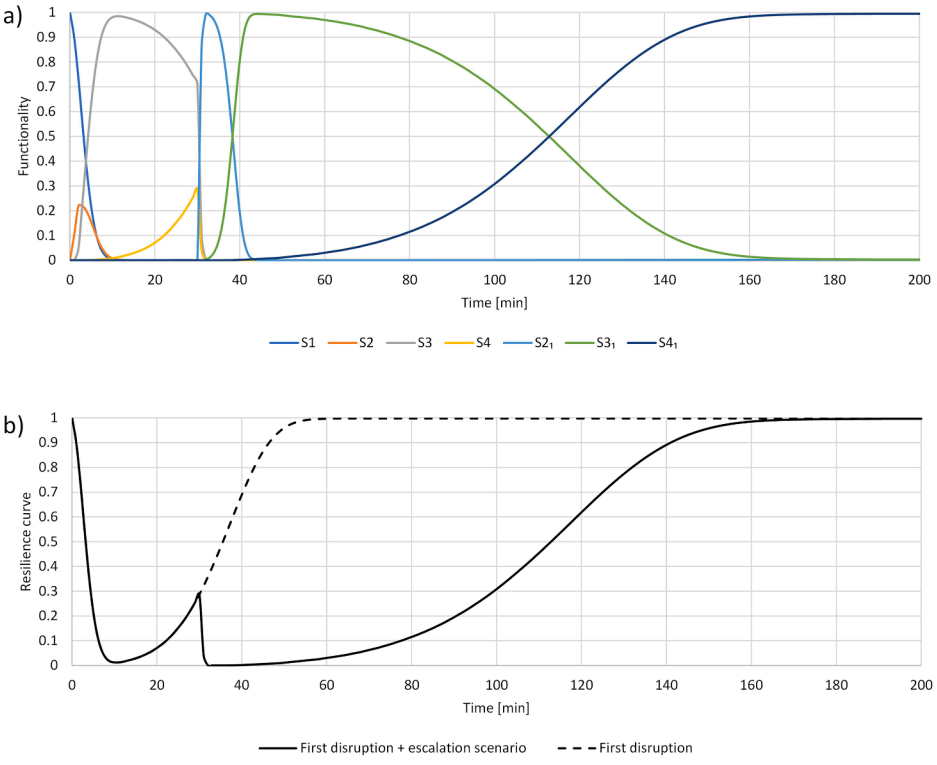

Fig. 10. a) Curves of functionality states of the examined case study (see Section 2.3 for the definition of the states); b) Dynamic resilience curve of the examined case study.

secondary equipment) requires replacement of the equipment that has a completely different time scale (days up to months). However, as stated above, this was not accounted in the case study carried out, that focuses on resolving the accident by minimizing consequences on people, assets, and the surrounding environment.

Examining in more detail the two lowest resilience values (i.e., the two relative minimums in the resilience curve), after the first disruption, the system resilience decreases until it reaches a value of 0.012 at 11 min, while the escalation scenario leads the system resilience to 0 in a few seconds: this means that the probability to be in a high functionality state ($S1$), or in a state in which the disruption is resolved, is close to 0. The reason for the more drastic decline after the escalation scenario is related to the latter, that exacerbates the compromised state of the system resulting from the first disruption. Furthermore, when the escalation scenario occurs, after 30 min from the first disruption, the probability of successful adaptation and restoration abilities of the system are 0.71 and 0.29, respectively, while the absorption ability is no more present (see curves $S3$, $S4$, and $S2$ in Fig. 10-a)) after 30 min.

Overall, Fig. 10 highlights the significant impact of the escalation scenarios on the system resilience and confirms the critical importance of safety measures and mitigation strategies aimed at preventing such escalations. It also highlights the importance of the robustness of emergency response plans and of the system inherent design to resist sequential failures. The difference between the two resilience curves in Fig. 10-b) underscores both the need to address singular incidents and to properly plan for the prevention and recovery from potential cascading effects that may critically affect the overall system resilience.

To further investigate the resilience of the LH_2 bunkering system analyzed, a posterior analysis was carried out, assuming specific basic events as evidence. The aim was to observe how the system behaves and restores when subjected to continuous solicitations or threats by specific elements. The failure of the ESD system, of the hydrogen leak detection devices, and the malfunction of the sprinklers were thus presumed as persistent system faults (evidence). In other words, nodes "*ESD*", "*Detection of H_2 leak*", and "*X32*" were set as follows: FAILURE = 1 and SUCCESS = 0, without considering in the analysis the occurrence probabilities of Table 3. The results obtained are reported in Fig. 11.

Under continuing system faults (evidence) affecting the adaptation attribute, the resilience curve (the dashed line in Fig. 11) tends to exhibit a lower capability to withstand disruptions. This is evident when comparing the resilience curves in case/not in case of evidence after 30 min. In the case of evidence, the probability of restoration from the jet-fire is lower compared to scenarios where theoretically no specific failures are present. Specifically, a resilience value of approximately 0.2 is observed in cases of evidence, in contrast to a value of 0.3 when no evidence is present. Additionally, restoration times result to be about 10 min longer in case of persistent failures, both for the single disruption scenario (dashed black line) and the escalation scenario (continuous black line). Although no significant increases in time were identified in the specific case study analyzed, such results show the potential for longer restoration times depending on the severity of the failures affecting the engineered system under investigation. Longer times can be obtained also if the system is in a low (L) state at the analysis time (refer to Section 2.3.3), due to its intrinsic degradation rate.

Future applications of the proposed model to various complex systems, such as Carbon Capture and Storage (CCS), shall allow the further assessment of the effectiveness and adaptability of the model across different contexts. This approach will help to strengthen the validation of the novel resilience model developed.

6. Conclusions

A novel quantitative model based on dynamic Bayesian network (DBNs) for the assessment of resilience of engineered systems in case of escalation scenarios caused by domino effects has been developed. The innovative resilience model has been then implemented into a systematic step-by-step procedure capable of evaluating the ability of complex systems to recover and restore functionality following the impact of cascading accident events. The results obtained allows a significant advancement in the assessment of engineered system resilience, filling the gap in the availability of a systematic quantitative procedure able to account for domino effects in both conventional and innovative infrastructure contexts. By leveraging the DBN framework, the novel approach developed is able to address the intricate temporal system dynamics inherent in resilience assessment, providing a comprehensive understanding of how resilience evolves over time when multiple accidental scenarios occur. Moreover, it handles uncertainty by adopting a probabilistic perspective, allowing for a more robust evaluation of resilience in the face of unpredictable events and disturbances. In doing so, this methodology equips stakeholders and decision-makers with valuable insights into the capability of engineered systems to recover to high functionality states, empowering them to proactively manage risks and enhance system performance in the face of escalating scenarios.

The application of the procedure to a case study in the context of LH_2 bunkering operations demonstrated the systematic nature of the step-by-step procedure, along with the ability of the resilience model to effectively handle escalation scenarios. The results highlight that the resilience of the system is strongly affected when the escalation scenario occurs in a system that is already damaged by the first disruption event. Furthermore, adaptation and restoration parameters, and system design are crucial for recovery, emphasizing the need for redundant safety barriers and improvement in maintenance.

Overall, the application of the proposed methodology to specific cryogenic bunkering operations demonstrated the quality of the results achievable in supporting human safety, protecting assets and the environment, and ensuring the continued operation and success of industrial operations in an increasingly uncertain and interconnected reality.

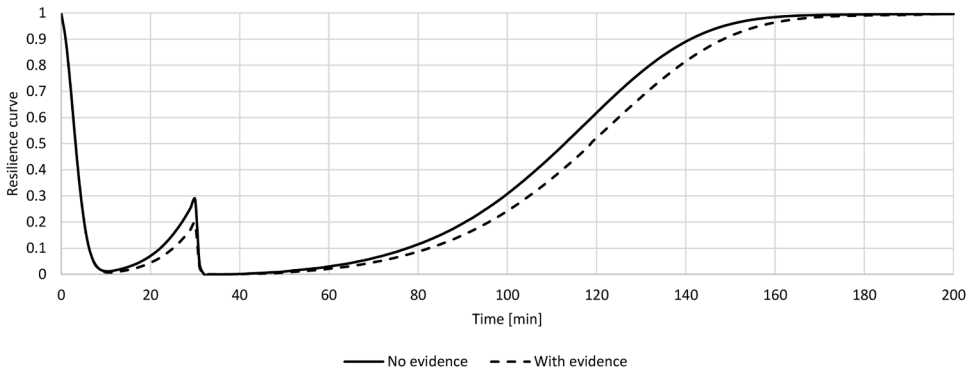

Fig. 11. Comparison between the dynamic resilience curves of the examined case study in case (dashed line) or not (solid line) of evidence.

AI Authors statement

During the preparation of this work the author(s) did not use any AI tool or service.

CRediT authorship contribution statement

Federica Tamburini: Writing – original draft, Methodology, Investigation, Conceptualization. **Matteo Iaiani:** Methodology, Investigation, Conceptualization. **Valerio Cozzani:** Writing – review & editing, Supervision, Conceptualization.

Declaration of competing interest

The authors declare that they have no known competing financial interests or personal relationships that could have appeared to influence the work reported in this paper.

Acknowledgments

Funding received from the Italian Ministry of University and Research under the National Recovery and Resilience Plan, Misson 4, Component 2, Investment 1.3, NextGenerationEU, Project "Network 4 Energy Sustainable Transition", PE00000021, CUPJ33C22002890007 is gratefully acknowledged.

This work was undertaken as part of the ELVHYS project (Project No 101101381) supported by the Clean Hydrogen Partnership and its members, funded by the European Union. UK participants in Horizon Europe Project ELVHYS are supported by UKRI (Grant No. 10063519 for the University of Ulster and Grant No. 10070592 for Health and Safety Executive). Views and opinions expressed are those of the authors only and do not necessarily reflect those of the European Union or of Clean Hydrogen JU. Neither the European Union nor the granting authority can be held responsible for them.

Appendix

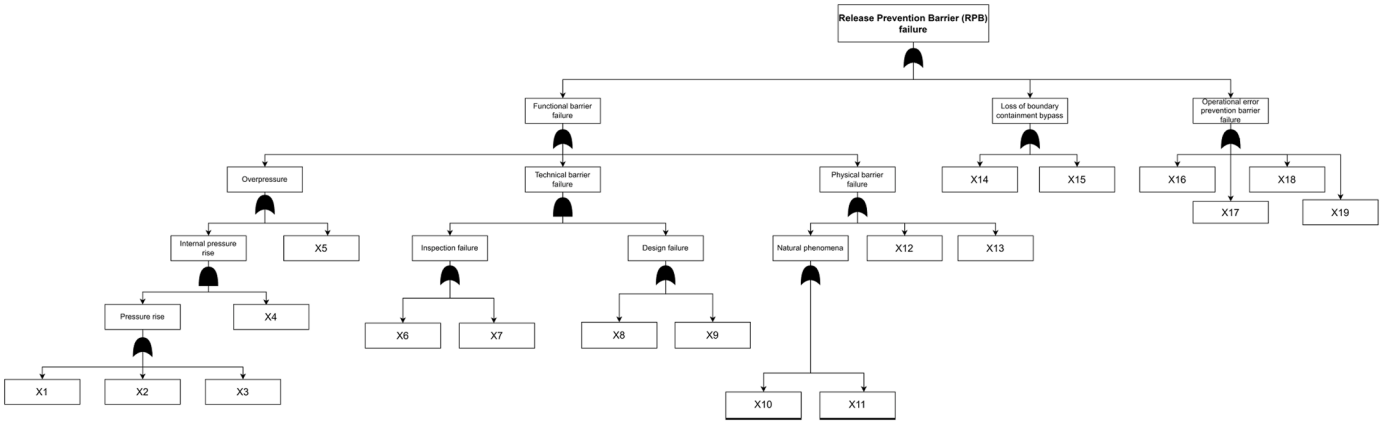

Fig. A.1. Fault tree of the Release Prevention Barriers (RPBs).

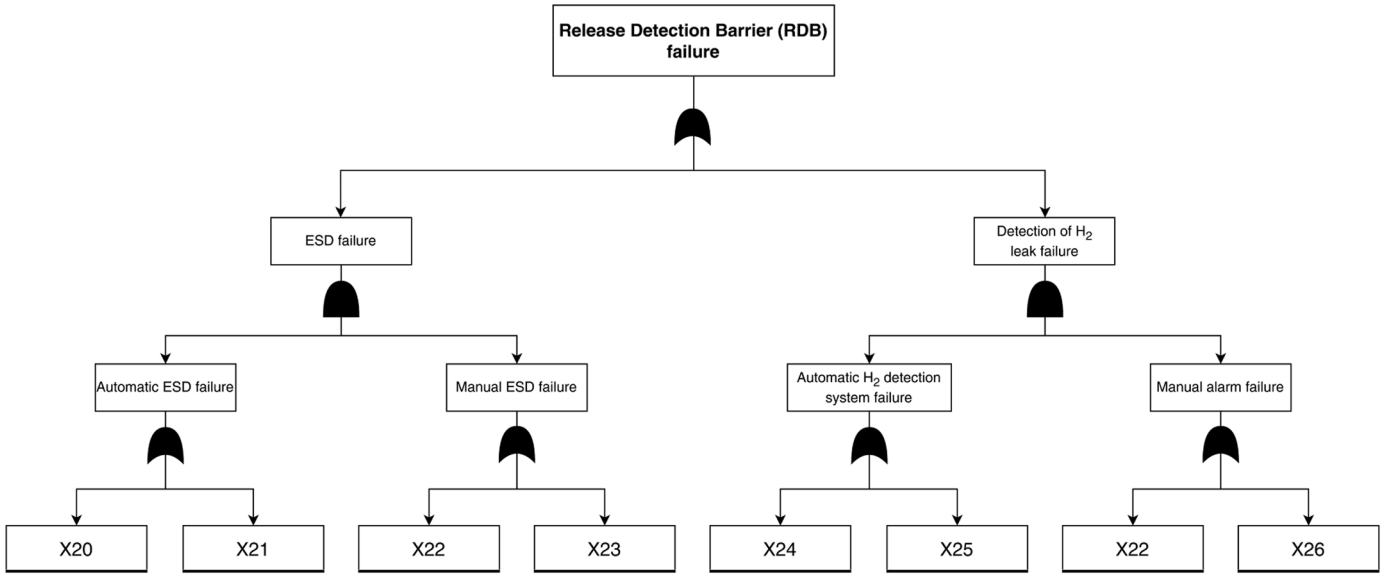

Fig. A.2. Fault tree of the Release Detection Barriers (RDBs).

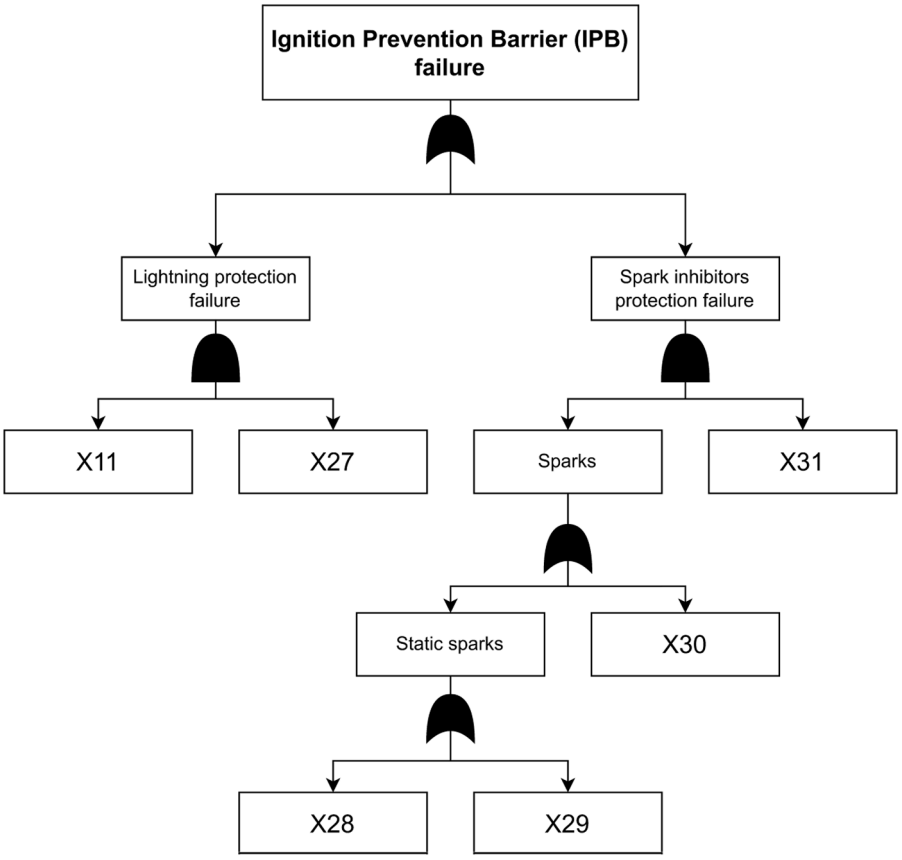

Fig. A.3. Fault tree of the Ignition Prevention Barriers (IPBs).

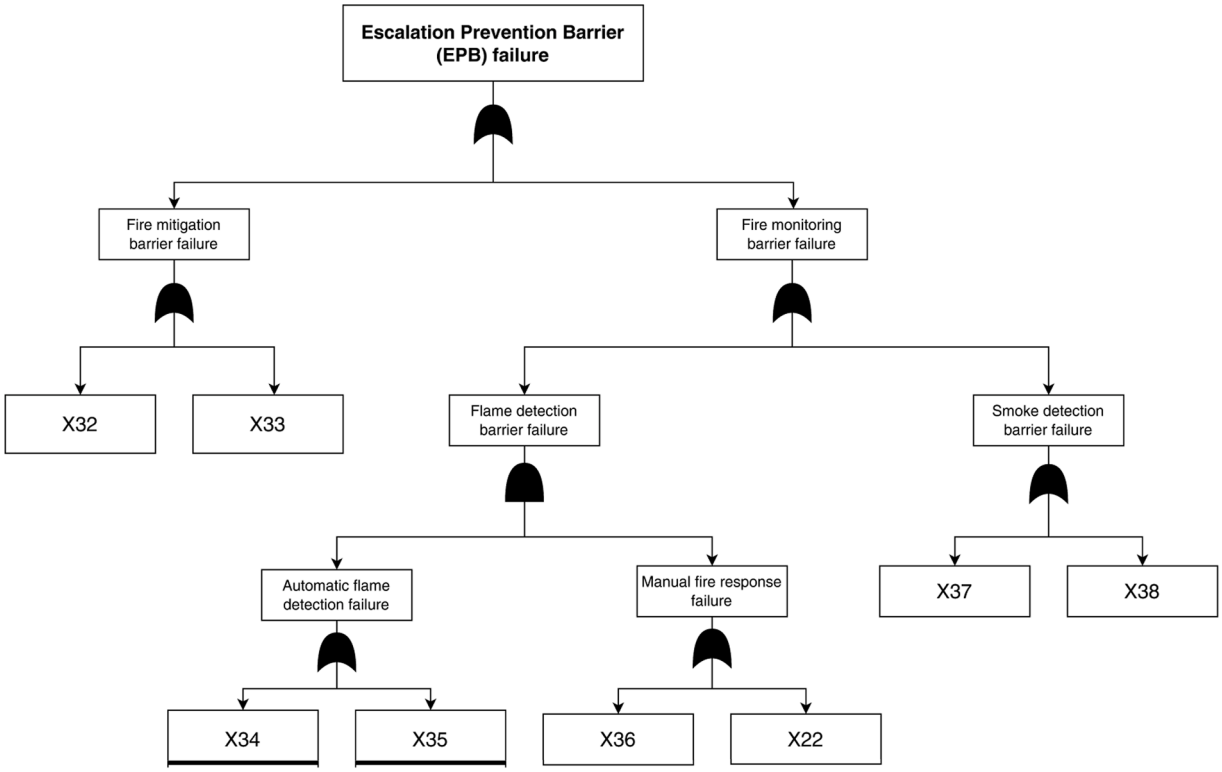

Fig. A.4. Fault tree of the Escalation Prevention Barriers (EPBs).

Data availability

Data will be made available on request.

References

[1] Wang J, Zuo W, Rhode-Barbarigos L, Lu X, Wang J, Lin Y. Literature review on modeling and simulation of energy infrastructures from a resilience perspective. Reliab Eng Syst Saf 2019;183:360–73. https://doi.org/10.1016/j.ress.2018.11.029.

[2] Tamburini F, Bonvicini S, Cozzani V. Consequences of subsea CO2 blowouts in shallow water. Process Saf Environ Prot 2024;183:203–16. https://doi.org/10.1016/j.psep.2024.01.008.

[3] Tamburini F, Zanobetti F, Cipolletta M, Bonvicini S, Cozzani V. State of the art in the quantitative risk assessment of the CCS value chain. Process Saf Environ Prot 2024;191:2044–63. https://doi.org/10.1016/j.psep.2024.09.066.

[4] Tamburini F, Bonvicini S, Cozzani V. Risk of subsea blowouts in marine CCS. Chem Eng Trans 2023;99:265–70. https://doi.org/10.3303/CET2399045.

[5] Tamburini F, Ricci F, Tzioutzios D, Paltrinieri N. Understanding Natech accident scenarios at carbon capture and storage (CCS) plants. Chem Eng Trans 2024;111:391–6. https://doi.org/10.3303/CET24111066.

[6] Tan Z, Wu B, Che A. Resilience modeling for multi-state systems based on Markov processes. Reliab Eng Syst Saf 2023;235. https://doi.org/10.1016/j.ress.2023.109207.

[7] Iaiani M, Tugnoli A, Cozzani V. Identification of cyber-risks for the control and safety instrumented systems: a synergic framework for the process industry. Process Saf Environ Prot 2023;172:69–82. https://doi.org/10.1016/j.psep.2023.01.078.

[8] Zio E. Challenges in the vulnerability and risk analysis of critical infrastructures. Reliab Eng Syst Saf 2016;152:137–50. https://doi.org/10.1016/j.ress.2016.02.009.

[9] Iaiani M, Fazari G, Tugnoli A, Cozzani V. Identification of reference security scenarios from past event datasets by Bayesian Network analysis. Reliab Eng Syst Saf 2025;254:110615. https://doi.org/10.1016/j.ress.2024.110615.

[10] Tong Q, Yang M, Zinetullina A. A Dynamic Bayesian Network-based approach to Resilience Assessment of Engineered Systems. J Loss Prev Process Ind 2020;65:104152. https://doi.org/10.1016/j.jlp.2020.104152.

[11] Gasser P, Lustenberger P, Cinelli M, Kim W, Spada M, Burgherr P, et al. A review on resilience assessment of energy systems. Sustain Resilient Infrastruct 2021;6:273–99. https://doi.org/10.1080/23789689.2019.1610600.

[12] Berkes F. Understanding uncertainty and reducing vulnerability: lessons from resilience thinking. Nat Hazards 2007;41:283–95. https://doi.org/10.1007/s11069-006-9036-7.

[13] Van Hoecke L, Laffineur L, Campe R, Perreault P, Verbruggen SW, Lenaerts S. Challenges in the use of hydrogen for maritime applications. Energy Environ Sci 2021;14:815–43. https://doi.org/10.1039/d0ee01545h.

[14] Khakzad S, Khan F, Abbassi R, Khakzad N. Accident risk-based life cycle assessment methodology for green and safe fuel selection. Process Saf Environ Prot 2017;109:268–87. https://doi.org/10.1016/j.psep.2017.04.005.

[15] Pawar B, Park S, Hu P, Wang Q. Applications of resilience engineering principles in different fields with a focus on industrial systems: a literature review. J Loss Prev Process Ind 2021;69:104366. https://doi.org/10.1016/j.jlp.2020.104366.

[16] Gu B., Liu J. A systematic review of resilience in the maritime transport. Int J Logist Res Appl n.d.:1–22. https://doi.org/10.1080/13675567.2023.2165051.

[17] Cozzani V, Gubinelli G, Antonioni G, Spadoni G, Zanelli S. The assessment of risk caused by domino effect in quantitative area risk analysis. J Hazard Mater 2005;127:14–30. https://doi.org/10.1016/j.jhazmat.2005.07.003.

[18] Li Y, Hu Z. Domino Effect Risk Assessment System for Offshore Oil and Gas Facilities Decommissioning. In: Proc. ASME 2022 41st Int. Conf. Ocean. Offshore Arct. Eng. Vol. 1 Offshore Technol.; 2022. https://doi.org/10.1115/OMAE2022-78196.

[19] Alileche N, Cozzani V, Reniers G, Estel L. Thresholds for domino effects and safety distances in the process industry: a review of approaches and regulations. Reliab Eng Syst Saf 2015;143:74–84. https://doi.org/10.1016/j.ress.2015.04.007.

[20] Abdolhamidzadeh B, Abbasi T, Rashtchian D, Abbasi SA. A new method for assessing domino effect in chemical process industry. J Hazard Mater 2010;182:416–26. https://doi.org/10.1016/j.jhazmat.2010.06.049.

[21] Morris M, Miles A, Cooper J. Quantification of escalation effects in offshore quantitative risk assessment. Morris MMiles ACooper J 1994;7:337–44. https://doi.org/10.1016/0950-4230(94)80047-2.

[22] Zeng T, Wei L, Reniers G, Chen G. A comprehensive study for probability prediction of domino effects considering synergistic effects. Reliab Eng Syst Saf 2024;251:110318. https://doi.org/10.1016/j.ress.2024.110318.

[23] Wang L, Huang R, Shi W, Zhang C. Domino effect in marine accidents: evidence from temporal association rules. Transp Policy 2021;103:236–44. https://doi.org/10.1016/j.tranpol.2021.02.006.

[24] Ustolin F, Campari A, Taccani R. An extensive review of liquid hydrogen in transportation with focus on the maritime sector. J Mar Sci Eng 2022;10. https://doi.org/10.3390/jmse10091222.

[25] Ab Rahim MS, Reniers G, Yang M, Bajpai S. Risk assessment methods for process safety, process security and resilience in the chemical process industry: a thorough literature review. J Loss Prev Process Ind 2024;88:105274. https://doi.org/10.1016/j.jlp.2024.105274.

[26] Patriarca R, Di Gravio G, Woltjer R, Costantino F, Praetorius G, Ferreira P, et al. Framing the FRAM: a literature review on the functional resonance analysis method. Saf Sci 2020;129:104827. https://doi.org/10.1016/j.ssci.2020.104827.

[27] Sun H, Yang M, Wang H. An integrated approach to quantitative resilience assessment in process systems. Reliab Eng Syst Saf 2024;243:109878. https://doi.org/10.1016/j.ress.2023.109878.

[28] Zinetullina A, Yang M, Khakzad N, Golman B, Li X. Quantitative resilience assessment of chemical process systems using functional resonance analysis method and Dynamic Bayesian network. Reliab Eng Syst Saf 2021;205:107232. https://doi.org/10.1016/j.ress.2020.107232.

[29] Yu J, Zeng Q, Yu Y, Zhang B, Ma W, Wu S, et al. Resilience assessment of FPSO leakage emergency response based on quantitative FRAM. Reliab Eng Syst Saf 2025;253:110526. https://doi.org/10.1016/j.ress.2024.110526.

[30] Jain P, Pasman HJ, Waldram S, Pistikopoulos EN, Mannan MS. Process Resilience Analysis Framework (PRAF): a systems approach for improved risk and safety management. J Loss Prev Process Ind 2018;53:61–73. https://doi.org/10.1016/j.jlp.2017.08.006.

[31] Hosseini S, Barker K. A Bayesian network model for resilience-based supplier selection. Int J Prod Econ 2016;180:68–87. https://doi.org/10.1016/j.ijpe.2016.07.007.

[32] Sun H, Wang H, Yang M, Reniers G. A STAMP-based approach to quantitative resilience assessment of chemical process systems. Reliab Eng Syst Saf 2022;222:108397. https://doi.org/10.1016/j.ress.2022.108397.

[33] Jain P, Rogers WJ, Pasman HJ, Keim KK, Mannan MS. A resilience-based integrated process systems hazard analysis (RIPSHA) approach: part I plant system layer. Process Saf Environ Prot 2018;116:92–105. https://doi.org/10.1016/j.psep.2018.01.016.

[34] Chen C, Yang M, Reniers G. A dynamic stochastic methodology for quantifying HAZMAT storage resilience. Reliab Eng Syst Saf 2021;215:107909. https://doi.org/10.1016/j.ress.2021.107909.

[35] Dhulipala SLN, Flint MM. Series of semi-Markov processes to model infrastructure resilience under multihazards. Reliab Eng Syst Saf 2020;193:106659. https://doi.org/10.1016/j.ress.2019.106659.

[36] Cincotta S, Khakzad N, Cozzani V, Reniers G. Resilience-based optimal firefighting to prevent domino effects in process plants. J Loss Prev Process Ind 2019;58:82–9. https://doi.org/10.1016/j.jlp.2019.02.004.

[37] Chen C, Reniers G, Yang M. A Resilience-Based Approach for the Prevention and Mitigation of Domino Effects. Saf. Secur. Sci. 2022;0:1–39. https://doi.org/10.1007/978-3-030-88911-1. Springer International Publishing.

[38] Tan Q, Chen G, Zhang L, Fu J, Li Z. Dynamic accident modeling for high-sulfur natural gas gathering station. Process Saf Environ Prot 2014;92:565–76. https://doi.org/10.1016/j.psep.2013.03.004.

[39] Caetano HO, LD N, Fogliatto MSS, Maciel CD. Resilience assessment of critical infrastructures using dynamic Bayesian networks and evidence propagation. Reliab Eng Syst Saf 2024;241:109691. https://doi.org/10.1016/j.ress.2023.109691.

[40] Jain P, Diangelakis NA, Pistikopoulos EN, Mannan MS. Process resilience based upset events prediction analysis: application to a batch reactor. J Loss Prev Process Ind 2019;62:103957. https://doi.org/10.1016/j.jlp.2019.103957.

[41] Jain P, Pistikopoulos EN, Mannan MS. Process resilience analysis based data-driven maintenance optimization: application to cooling tower operations. Comput Chem Eng 2019;121:27–45. https://doi.org/10.1016/j.compchemeng.2018.10.019.

[42] Iaiani M, Musayev N, Tugnoli A, Macini P, Mesini E, Cozzani V. Identification of security scenarios in offshore Oil&Gas production facilities based on past incident analysis. Process Saf Environ Prot 2024;192:926–45. https://doi.org/10.1016/j.psep.2024.10.061.

[43] Iannacone L, Sharma N, Tabandeh A, Gardoni P. Modeling time-varying reliability and resilience of deteriorating infrastructure. Reliab Eng Syst Saf 2022;217:108074. https://doi.org/10.1016/j.ress.2021.108074.

[44] Tabandeh A, Sharma N, Gardoni P. Uncertainty propagation in risk and resilience analysis of hierarchical systems. Reliab Eng Syst Saf 2022;219:108208. https://doi.org/10.1016/j.ress.2021.108208.

[45] Vairo T, Gualeni P, Reverberi AP, Fabiano B. Resilience dynamic assessment based on precursor events: application to ship lng bunkering operations. Sustain 2021;13. https://doi.org/10.3390/su13126836.

[46] Liu Y, Ma X, Qiao W, Ma L, Han B. A novel methodology to model disruption propagation for resilient maritime transportation systems–a case study of the Arctic maritime transportation system. Reliab Eng Syst Saf 2024;241:109620. https://doi.org/10.1016/j.ress.2023.109620.

[47] Sun H, Yang M, Zio E, Li X, Lin X, Huang X, et al. A simulation-based approach for resilience assessment of process system: a case of LNG terminal system. Reliab Eng Syst Saf 2024;249:110207. https://doi.org/10.1016/j.ress.2024.110207.

[48] Hu J, Khan F, Zhang L. Dynamic resilience assessment of the Marine LNG offloading system. Reliab Eng Syst Saf 2021;208:107368. https://doi.org/10.1016/j.ress.2020.107368.

[49] Claussner L, Ustolin F. System resilience of a liquid hydrogen terminal during loading and unloading operations. IFAC-PapersOnLine 2024;58:359–64. https://doi.org/10.1016/j.ifacol.2024.08.147.

[50] Khakzad N. Application of dynamic Bayesian network to risk analysis of domino effects in chemical infrastructures. Reliab Eng Syst Saf 2015;138:263–72. https://doi.org/10.1016/j.ress.2015.02.007.

[51] Chang J, Bai Y, Xue J, Gong L, Zeng F, Sun H, et al. Dynamic Bayesian networks with application in environmental modeling and management: a review. Environ Model Softw 2023;170:105835. https://doi.org/10.1016/j.envsoft.2023.105835.

[52] Zeng L, Ge Z. Bayesian network for dynamic variable structure learning and transfer modeling of probabilistic soft sensor. J Process Control 2021;100:20–9. https://doi.org/10.1016/j.jprocont.2021.02.004.

[53] Zinetullina A, Yang M, Khakzad N, Golman B. Dynamic resilience assessment for process units operating in Arctic environments. Saf Extrem Environ 2020;2:113–25. https://doi.org/10.1007/s42797-019-00008-3.
[54] Jensen F.V., Nielsen T.D. Bayesian networks and decision graphs. Statistics for engineering and information science. 2007.
[55] Ibrahim H, Patruni JR. Bayesian network-based failure analysis of fire safety barriers in floating LNG facility. SN Appl Sci 2019;1:1–17. https://doi.org/10.1007/s42452-019-1106-z.
[56] Devarakonda N, Pamidi S, Kumari VV, Govardhan A. Intrusion detection system using bayesian network and hidden Markov model. Procedia Technol 2012;4:506–14. https://doi.org/10.1016/j.protcy.2012.05.081.
[57] Tran HT, Balchanos M, Domerçant JC, Mavris DN. A framework for the quantitative assessment of performance-based system resilience. Reliab Eng Syst Saf 2017;158:73–84. https://doi.org/10.1016/j.ress.2016.10.014.
[58] Ouyang M, Dueñas-Osorio L, Min X. A three-stage resilience analysis framework for urban infrastructure systems. Struct Saf 2012;36–37:23–31. https://doi.org/10.1016/j.strusafe.2011.12.004.
[59] Yodo N, Wang P, Zhou Z. Using Dynamic Bayesian Networks. IEEE Trans Reliab 2017;66:1–10. https://doi.org/10.1109/TR.2017.2722471.
[60] Francis R, Bekera B. A metric and frameworks for resilience analysis of engineered and infrastructure systems. Reliab Eng Syst Saf 2014;121:90–103. https://doi.org/10.1016/j.ress.2013.07.004.
[61] Rathnayaka S, Khan F, Amyotte P. SHIPP methodology: predictive accident modeling approach. Part I: methodology and model description. Process Saf Environ Prot 2011;89:151–64. https://doi.org/10.1016/j.psep.2011.01.002.
[62] Reniers G, Cozzani V. Domino effects in the process industries: modelling. Prevention and Managing 2013:1–372.
[63] Trivedi KS, Bobbio A. Non-homogeneous continuous-time Markov chains. Reliab. Availab. Eng. 2017:489–508. https://doi.org/10.1017/9781316163047.018.
[64] Farrell S, Ludwig CJH. Bayesian and maximum likelihood estimation of hierarchical response time models. Psychon Bull Rev 2008;15:1209–17. https://doi.org/10.3758/PBR.15.6.1209.
[65] Serfozo R. Continuous-time Markov Chains. In: Springer-Verlag, editor. Basics appl. stoch. process. probab. its appl., Berlin: 2009, p. 241–2.
[66] Trivedi KS, Bobbio A. State-space models with exponential distributions. Reliab. Availab. Eng. 2017:303–4. https://doi.org/10.1017/9781316163047.012.
[67] TNO. Red book: methods for determining and processing probabilities. 2005.
[68] Lees' Mannan S. Loss prevention in the process industries. Elsevier; 2012. https://doi.org/10.1016/b978-0-12-397189-0.00001-x.
[69] Go HY, Il Sung S, Kim YS. Prediction of system reliability using failure types of components based on Weibull lifetime distribution. J Mech Sci Technol 2018;32:2463–71. https://doi.org/10.1007/s12206-018-0503-3.
[70] Kumar AR, V K. A Study on system reliability in Weibull distribution. Ijireeice 2017;5:38–41. https://doi.org/10.17148/ijireeice.2017.5308.
[71] Song Y, Li R. System resilience distribution identification and analysis based on performance processes after disruptions. PLoS One 2022;17:1–21. https://doi.org/10.1371/journal.pone.0276908.
[72] Paprocka I, Kempa WM, Ćwikła G. Predictive maintenance scheduling with failure rate described by truncated normal distribution. Sensors (Switzerland) 2020;20:1–23. https://doi.org/10.3390/s20236787.
[73] British Standards Institution. Hazard and operability studies (HAZOP studies): application guide., 2016.
[74] Tamburini F, Ustolin F, Cozzani V, Paltrinieri N. Performance assessment of safety barriers in liquid hydrogen bunkering operations using bayesian network. In: Proc. ASME 2024 43rd Int. Conf. Ocean. Offshore Arct. Eng. OMAE2024, June 9-14, 2024, Singapore, Singapore; 2024. p. 1–9. https://doi.org/10.1115/OMAE2024-126832.
[75] SINTEF. The offshore and onshore reliability data OREDA 2022.
[76] HUGIN EXPERT A/S. Hugin 2024.
[77] BayesFusion. GeNIe Modeler 2024.
[78] Murphy KP. Dynamic bayesian networks. In: NIPS 2006 Proc. 19th Int. Conf. Neural Inf. Process. Syst.; 2002. https://doi.org/10.7551/mitpress/7503.003.0056.
[79] Tamburini F, Ustolin F, Salzano E, Cozzani V, Paltrinieri N. Lessons learned from experimental tests concerning liquid hydrogen releases. Inst. Chem. Eng. Symp. Ser. 2023.
[80] Tamburini F, Sgarbossa F, Cozzani V, Paltrinieri N. Task analysis and human error identification to improve the liquid hydrogen bunkering process in the maritime sector. Proc. ESREL2023 2023;2050:647–54. https://doi.org/10.3850/978-981-18-8071-1_p492-cd.
[81] Moss Maritime. Liquid hydrogen bunker vessel. 2019.
[82] Tofalos C, Jeong B, Jang H. Safety comparison analysis between LNG/LH2 for bunkering operation. J Int Marit Saf Environ Aff Shipp 2020;4:135–50. https://doi.org/10.1080/25725084.2020.1840859.
[83] Correa-Jullian C, Groth KM. Data requirements for improving the quantitative risk assessment of liquid hydrogen storage systems. Int J Hydrogen Energy 2022;47:4222–35. https://doi.org/10.1016/j.ijhydene.2021.10.266.
[84] Ødegård A., Sommerseth C., Odsæter L.H., Skarsvåg H.L., Nekså P., Meraner C., et al. D5.4: SH2IFT final project report. 2022.
[85] van Wingerden K, Kluge M, Habib AK, Skarsvåg HL, Ustolin F, Paltrinieri N, et al. Experimental Investigation into the Consequences of Release of Liquified Hydrogen onto and under Water. Chem Eng Trans 2022;90:541–6. https://doi.org/10.3303/CET2290091.
[86] Tamburini F, Kluge M, Habib AK, Ustolin F, Cozzani V, Paltrinieri N. Exploring experimental tests concerning liquid hydrogen releases. Process Saf Environ Prot 2024;192:1330–43. https://doi.org/10.1016/j.psep.2024.11.014.
[87] Verfondern K, Dienhart B. Pool spreading and vaporization of liquid hydrogen. Int J Hydrogen Energy 2007;32:256–67. https://doi.org/10.1016/j.ijhydene.2006.01.016.
[88] Gómez-Mares M, Muñoz M, Palacios A. Jet fires: a "minor" fire hazard joaquim casal. Chem Eng Trans 2012;26:13–20. https://doi.org/10.3303/CET1226003.
[89] van Wingerden K, Kluge M, Habib AK, Ustolin F, Paltrinieri N. Medium-scale tests to investigate the possibility and effects of BLEVEs of storage vessels containing liquified hydrogen. Chem Eng Trans 2022;90:547–52. https://doi.org/10.3303/CET2290092.
[90] Salzano E, Picozzi B, Vaccaro S, Ciambelli P. Hazard of pressurized tanks involved in fires. Ind Eng Chem Res 2003;42:1804–12. https://doi.org/10.1021/ie020606r.
[91] Iaiani M, Tugnoli A, Cozzani V, Reniers G, Yang M. A Bayesian-network approach for assessing the probability of success of physical security attacks to offshore Oil&Gas facilities. Ocean Eng 2023;273:114010. https://doi.org/10.1016/j.oceaneng.2023.114010.
[92] Taylor C, Øie S, Paltrinieri N. Human reliability in the petroleum industry: a case study of the petro-HRA method. Risk. Reliab Saf Innov Theory Pract - Proc 26th Eur Saf Reliab Conf ESREL 2016;2017:162. https://doi.org/10.1201/9781315374987-152.
[93] Gertman DI, Blackman HS, Marble JL, Smith C, Boring RL, O'Reilly P. The SPAR H human reliability analysis method. In: Am Nucl Soc 4th Int Top Meet Nucl Plant Instrumentation, Control Hum Mach Interface Technol; 2004. p. 17–24.
[94] Garcia M.L. Design and evaluation of physical protection systems: second edition. 2007. https://doi.org/10.1016/C2009-0-25612-1.